Surface modification of sulfur pre-vulcanized natural rubber (SPNR) sheets using bismuth oxyiodide (BiOI) microparticles and polymethyl methacrylate (PMMA)

Pathitta Kongthong

Advisor

Assistant Professor Dr. Teeraporn Suteewong

A Report Submitted in Partial Fulfillment of the Requirements

for the Degree of Bachelor of Engineering (Petrochemical Engineering),

Department of Chemical Engineering, Faculty of Engineering,

King Mongkut's Institute of Technology Ladkrabang

Academic Year 2019

การปรับปรุงพื้นผิวโดยการสังเคราะห์อนุภาคโลหะบิสมัส ออกซิไอโอไดด์ (BiOI) และพอลิเมทิล เมทาคริเลต (PMMA) บนแผ่นยางธรรมชาติพรีวัลคาไนซ์ (SPNR)

ปทิตตา กองทอง

อาจารย์ที่ปรึกษา

ผู้ช่วยศาสตราจารย์ ดร. ธีรพร สุธีวงศ์

ปริญญานิพนธ์นี้เป็นส่วนหนึ่งของการศึกษาตามหลักสูตรวิศวกรรมศาสตร์บัณฑิต

สาขาวิชาวิศวกรรมปิโตรเคมีภาควิชาวิศวกรรมเคมี คณะวิศวกรรมศาสตร์

สถาบันเทคโนโลยีพระจอมเกล้าเจ้าคุณทหารลาดกระบัง

ปีการศึกษา 2562

Title	Surface modification of sulfur pre-vulcanized natural rubber (SPNR) sheets using bismuth oxyiodide (BiOI) microparticles and polymethyl methacrylate (PMMA)
By	Pathitta Kongthong
Field of Study	Petrochemical Engineering
Advisor	Asst. Prof. Dr. Teeraporn Suteewong

Accepted by the Faculty of Engineering, King Mongkut's Institute of Technology Ladkrabang in Partial Fulfillment of the Requirements for the Degree of Bachelor of Engineering (Petrochemical Engineering).

Thesis Committee

TEERAPORN Chairman
(Asst. Prof. Dr. Teeraporn Suteewong)

Committee
(Assoc. Prof. Dr. Duangkamol Na-Ranong)

Yaneeporn Committee
(Asst. Prof. Dr. Yaneeporn Patcharavorachot)

Title	Surface modification of sulfur pre-vulcanized natural rubber (SPNR) sheets using bismuth oxyiodide (BiOI) microparticles and polymethyl methacrylate (PMMA)
By	Pathitta Kongthong
Advisor	Asst. Prof. Dr. Teeraporn Suteewong
Field of Study	Petrochemical Engineering
Affiliation	Department of Chemical Engineering, Faculty of Engineering, King Mongkut's Institute of Technology Ladkrabang

Abstract

Surface modification of sulfur pre-vulcanized natural rubber (SPNR) sheet has been performed by the formation of poly(methyl methacrylate) (PMMA) and synthesis of bismuth oxyiodide (BiOI) microparticles on the surface at low temperature in aqueous system. SPNR sheet was first immersed in MMA emulsion. BiOI was then formed on MMA-swollen SPNR by mixing bismuth(III) nitrate pentahydrate ($Bi(NO_3)_3.5H_2O$) and potassium iodide (KI). Effect of KI concentration, pH and dipping time were studies. Morphologies and amount of BiOI/PMMA-coated SPNR sheet were observed by scanning electron microscopy with energy-dispersive X-ray spectroscopy (SEM/EDX). The obtained 3D structure BiOI microparticles/PMMA-modified SPNR sheets were characterized by X-ray diffraction (XRD), thermogravimetric analyzer (TGA) and Fourier-transform infrared spectroscopy (FT-IR). The photodegradation of stearic acid (SA) was investigated using FT-IR technique. It was found that the 3D structure flower-like BiOI microparticles/PMMA modified SPNR exhibits high photocatalytic activity.

Keywords: Natural rubber, Poly(methyl methacrylate), Bismuth, Bismuth oxyhalide

เรื่อง การปรับปรุงพื้นผิวโดยการสังเคราะห์อนุภาคโลหะบิสมัส ออกซิไอโอไดด์ (BiOI) และพอลิเมทิล เมทาคริเลต (PMMA) บนแผ่นยางธรรมชาติพรีวัลคาไนซ์ (SPNR)

โดย ปทิตตา กองทอง

อาจารย์ที่ปรึกษา ผศ.ดร. ธีรพร สุธีวงศ์

สาขาวิชา วิศวกรรมปิโตรเคมี

สังกัด ภาควิชาวิศวกรรมเคมี คณะวิศวกรรมศาสตร์
สถาบันเทคโนโลยีพระจอมเกล้าเจ้าคุณทหารลาดกระบัง

บทคัดย่อ

งานวิจัยนี้ทำการปรับปรุงพื้นผิวของแผ่นฟิล์มยางธรรมชาติที่ผ่านกระบวนการพรีวัลคาไนซ์ด้วยซัลเฟอร์ (SPNR) โดยการสังเคราะห์พอลิเมทิลเมทาคริเลต (PMMA) และอนุภาคบิสมัส ออกซิไอโอไดด์ (BiOI) บนผิวยางที่อุณหภูมิต่ำเป็นเวลา 6 ชั่วโมง ในสารละลายที่มีน้ำเป็นตัวทำละลาย โดยเริ่มจากการจุ่มแผ่นยางลงในสารละลายอิมัลชันของเมทิลเมทาคริเลต (MMA) แล้วทำการสังเคราะห์อนุภาคบิสมัส ออกซิไอโอไดด์ลงบนแผ่นยาง โดยการจุ่มแผ่นยางลงในสารละลายผสมของบิสมัท(III) ไนเตรท เพนตะไฮเดรต ($Bi(NO_3)_3.5H_2O$) และโพแทสเซียม ไอโอไดด์ (KI) และการศึกษาผลของความแตกต่างของความเข้มข้นของโพแทสเซียม ไอโอไดด์ เวลาในการจุ่มยาง และ pH ของสารละลาย รวมถึงทำการศึกษาโครงสร้างสัณฐานวิทยา และจำนวนของอนุภาคบิสมัส ออกซิไอโอไดซ์บนยาง ด้วยกล้องจุลทรรศน์อิเล็กตรอนแบบส่องกราด และการวิเคราะห์องค์ประกอบทางเคมีด้วยสเปกโทรเมทรีรังสีเอกซ์แบบกระจายพลังงาน (SEM/EDX). ศึกษาลักษณะของอนุภาคบิสมัส ออกซิไอโอไดด์ บนแผ่นยางที่เตรียมได้โดยเครื่องวิเคราะห์การเลี้ยวเบนของรังสีเอ็กซ์ (XRD) การวิเคราะห์การเปลี่ยนแปลงน้ำหนักของสารโดยอาศัยคุณสมบัติทางความร้อน (TGA) และเครื่องมือสำหรับวิเคราะห์หาชนิดและปริมาณสาร โดยการวัดการดูดกลืนแสงของสารในช่วงอินฟาเรด (FT-IR) และศึกษาสมบัติการการย่อยสลายด้วยแสง โดยการย่อยสลายกรดสเตียริก พบว่ามีคุณสมบัติการการย่อยสลายด้วยแสงที่ดี

คำสำคัญ: ยางธรรมชาติ, พอลิเมทิลเมทาคริเลต, อนุภาคบิสมัส, บิสมัส ออกซิเฮไลด์

Acknowledgements

I am extremely thankful and pay my gratitude to my advisor Asst Prof. Dr. Teeraporn Suteewong for imparting her knowledge, her valuable guidance with me and support for completion of this project. Without her continuous encouragement and support in every section of this project, it would be hardly to complete.

I will not forget to thank every instrument staff for giving information and teach me about preparing of sample, instrument operation and analysis.

I would like to express my special gratitude toward my family who is always by my side when I need their help and thank you for their encouragement.

Finally, I would like to thank all of my friend who directly or indirectly helped me to complete this project.

Pathitta Kongthong

Table of Contents

List of Figures

List of Tables

CHAPTER I

INTRODUCTION

1.1 Background

Natural rubber latex (NRL) is natural colloidal polymer which consists of rubber molecules or cis-1,4-polyisoprene, water, fatty acids, phospholipid and protein. Due to its high elasticity and good mechanical properties, NRL, after pre-vulcanized, has been used as in thin film especially gloves. After fabrication, the surface of NRL-based products must be treated to lower surface friction. Talc or other powder have commonly been used to coat the surface of NR products. However, as physically adhered, these powders can cause contamination and allergy, Alternative surface treatment that can both improve and modify the properties of NR-based products is interesting.

Chemical modification of the surface of NR products can be done in various ways such as plasma treatment, grafting and attachment of particles. Covalently fabricating nanoparticles on the rubber surface could improve surface friction as well as introduce new properties to NR, depending on type of nanoparticles. Anancharungsuk et al. coated the cationic surface of polyacrylamide-grafted sulphur pre-vulcanized NR (SPNR) with anionic poly (methyl methacrylate) (PMMA) via the electrostatic interaction. [1,2,3] It was found that surface roughness (R_a) of the coated SPNR increased and surface friction decreased. This modified rubber films also showed no toxicity against L-929 fibroblasts. Modifying the surface of PMMA particles with chitosan or its derivative, before coating the rubber surfaces, not only altered of R_a and surface friction, antibacterial properties of SPNR also improved due to the antibacterial of chitosan. [4,5] There are also metal and metal oxide, such as silver (Ag), zinc oxide (ZnO) and titanium dioxide (TiO_2), that provide superior antimicrobial activity. Ag and chitosan coated NR particles showed the higher antibacterial properties of modified NR than using only chitosan. [6,7] These works illustrate the extension of these modified NR as hygienic or healthcare-related products especially in hospitals or senior houses.

Although ZnO is considered as effective antibacterial, it is harmful to marine organism. TiO_2 is very effective photocatalyst, low cost and low toxic. However, due to its large band gap (3.2 eV), it can effectively be active under the UV region. The metal compound with lower band gap (< 3.0 eV) includes bismuth tungstate (Bi_2WO_6), bismuth titanate, bismuth

vanadate (Bi_2VO_4), bismuth oxybromide (BiOBr), bismuth oxyiodide (BiOI), silver nanoparticles ($AgWO_3$) and some copper compound nanoparticles. Among these, bismuth-based nanoparticles show cost effective, broad spectrum, antimicrobial, antibacterial and non-toxic in UV, visible and fluorescent light. [8,9] In order to lower the cost of Ag and broaden the antibacterial function under broad spectrum of radiation, bismuth-based nano/microparticles are interesting candidate.

In this work, we aim to modify the surface of SPNR sheets by forming bismuth complex nanoparticles on PMMA-modified SPNR using induced redox/Emulsion polymerization. SPNR sheets was first immersed in MMA emulsion containing purified MMA, tert-Butyl hydroperoxide (*t*-BuHP), and sodium dodecyl sulphate (SDS). Then, MMA-swollen SPNR sheets was dipped in bismuth precursor ($Bi(NO)_3.5H_2O$) solution before adding KI solution. The polymerization reaction preformed in aqueous solution of fructose and ferrous ion at 60°C for 6 hours. Effect of immersion times, pH of BiOI solution and concentration of KI precursor on the formation of BiOI and PMMA particles will be investigated using scanning electron microscopy with energy dispersive X-ray spectroscopy (SEM/EDX), X-Ray diffractometer (XRD), Thermogravimetric analyzer (TGA) and Fourier-transform infrared spectroscopy (FT-IR). Photocatalytic activities of or BiOI microparticles/PMMA-modified SPNR sheets will be considered by estimating the reduction of stearic acid (SA) on modified surface using FT-IR technique. [10] Morphologies of BiOI particles embedded on PMMA-modified SPNR sheets will also be discussed.

1.2 Objectives

1.2.1 To synthesize bismuth oxyiodide (BiOI) particles and PMMA on the surface of SPNR sheet.

1.2.2 To investigate the photodegradation properties of the modified-SPNR sheets under UV light region.

1.3 Scopes of Work

1.3.1 Synthesis of BiOI microparticles/PMMA- modified SPNR sheets using induced redox/Emulsion polymerization technique.

1.3.2 Characterization of BiOI microparticles /PMMA-modified SPNR sheets

- Scanning electron microscopy with energy dispersive X-ray spectroscopy (SEM/ EDX)
- X-Ray diffractometer (XRD)
- Thermogravimetric analyzer (TGA)
- Fourier-transform infrared spectroscopy (FTIR)

1.3.3 Photodegradation activities test using Fourier-transform infrared spectroscopy (FTIR).

1.4 Expected output

1.4.1 BiOI microparticles can be uniformly adhere on surface of SPNR sheet.

1.4.2 Photodegradation activities of BiOI microparticles /PMMA-modified SPNR sheets under UV light region is enhanced.

CHAPTER II

LITERATURE REVIEW

2.1 Interpenetrating Polymer Networks (IPNs)

The interpenetrating polymer networks (IPNs) are type of polymer surface modification in which two chemically district networks are miscible mixed to form network chains as interlocking network (catenanes). The catenanes is two or more interlocked ring which interlocked macrocycle cannot be separated excluding breaking of covalent bond. IPNs are generally categorized as full IPNs and semi IPNs, relying on one or two cross-linked components.[11]

The commonly synthesis of IPNs method consists of simultaneous IPN and sequential IPN. The IPNs is synthesized by simultaneously or sequent polymerization and crosslinking of two monomers with low phase separation due to rapidly increasing viscosity. The sequential IPN is the polymerization of two polymer networks that does not occurred at the same time. [12] The monomer and crosslinking agent are swollen in polymer network before second polymerization. In organic and inorganic case, the organic can be polymerized to form organic networks before inorganic networks. A second route, monomers are dissolved and polymerized into polymer network to crosslinked second interpenetrating network. Two polymers are blended and thermodynamically miscible that crosslinking come after in final route. Phase separation of particle proceed during IPNs formation due to different chemical structure components lead to heterogenous structure which would break IPNs formation. The phase separation forms, therefore IPNs are not occurred.

A 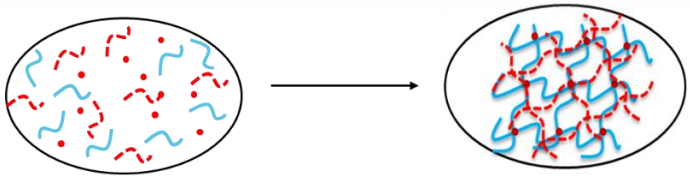

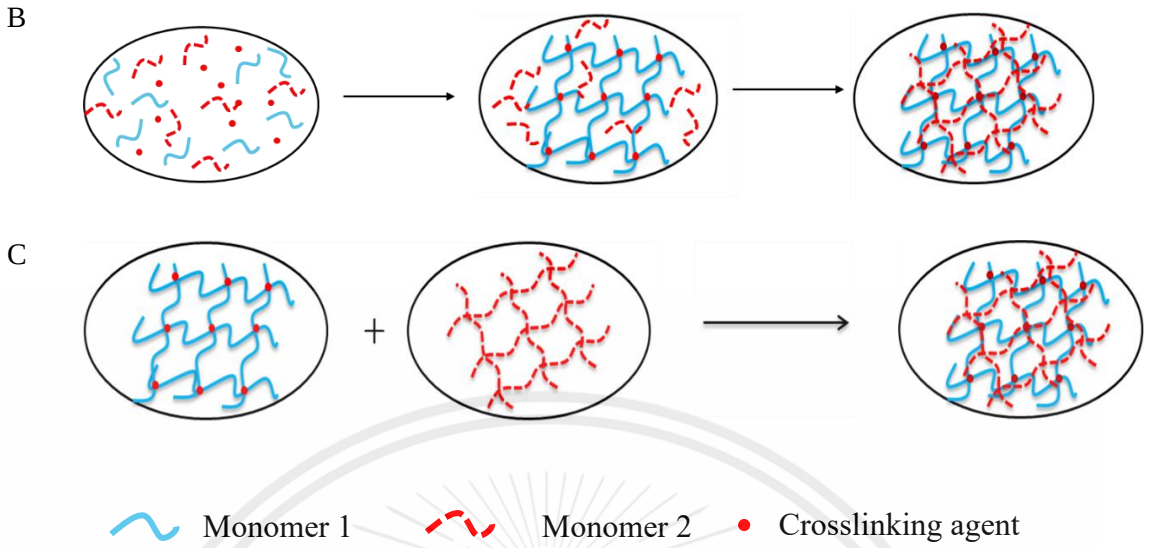

Figure 2.1 Synthesis of IPNs: (A) Simultaneous IPN, (B) Sequential IPN and (C) Interpenetrating polymer networks from two polymer blending.

2.1.1 Full interpenetrating polymer networks (IPNs)

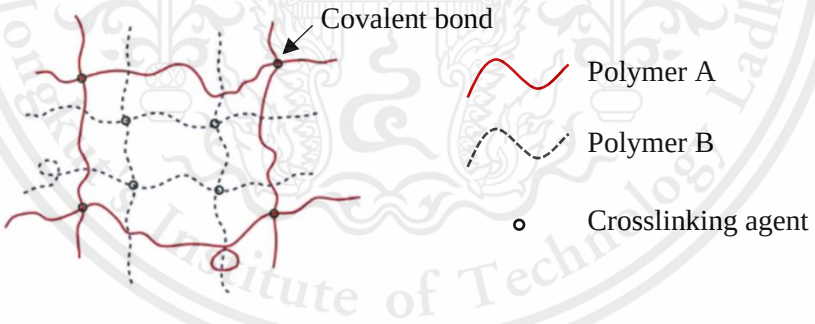

Figure 2.2 Full interpenetrating polymer networks (Full-IPNs)

Full interpenetrating polymer networks (Full-IPNs) is the polymer contains two or more polymer in network, which is partially interlaced on molecular scale as shows in **Figure 2**. Each molecule network has no covalent bonding to the other. This polymer networks cannot be separated excluding breaking of chemical bonding. Two polymers blending with no interlacing network is not defined to IPNs. [13]

2.1.2 Semi-Interpenetrating Polymer Networks (SIPNs)

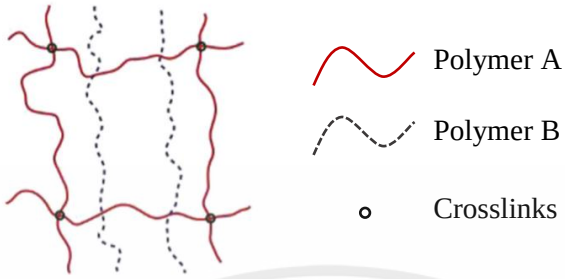

Figure 2.3 Semi-interpenetrating polymer networks (SIPNs)

Semi-interpenetrating polymer networks (SIPNs) or pseudo-interpenetrating polymer networks are the combination of one polymer network and one or more monomer or branched of polymers as shown in **Figure 3.** The distinction of SIPNs from IPNs is combination of branched of polymer and polymer without forming interpenetrated network and branched of polymer can be separated from polymer networks without chemical bonding. The IPN is represented as crosslinked network but, the SIPN is represented only one polymer as a network. The formation of SIPNs increases miscibility in comparison with full IPNs. [13,14]

2.1.3 Properties and application of interpenetrating polymer networks (IPNs) and semi interpenetrating polymer networks (SIPNs)

Interpenetrating polymer networks (IPNs) lead to intimate mixing of phase, smaller domain sizes, damping properties than blending which is physical mixed of two polymers and better mechanical properties such as increasing phase stability of product, high thermo-stability, better mechanical properties, chemical resistance, excellent dielectric properties, radar transparency and nutrient permeability etc. [12,14]

2.2 Bismuth micro/nanoparticles (Bi)

2.2.1 General information of bismuth micro/nanoparticles (Bi)

The attractive property of bismuth nanoparticle is its photocatalytic activity under visible light. Many photocatalyst is restricted due to poor visible light absorption which in results of wide band gap. Photocatalyst with narrow band gap is then attractive (less than 3.0 eV). Most bismuth complexed nanoparticles have band gap smaller than 3.0 eV, especially bismuth sulfide (Bi_2S_3) which has band gap less than 2.0 eV. [15] The interested properties of bismuth nanoparticles are broad spectrum, highly effective, low cost and lower toxic side effect. The important characteristic of Bi is non-toxic for human cell which Bi-NPs is considered one of the least toxic of the heavy metals for industrial and minimum treat to the environment. [16] The family of bismuth (Bismuth metallates) such as bismuth tungstate (Bi_2WO_6), bismuth vanadate (Bi_2VO_4), bismuth titanute, bismuth molybdenum oxide (Bi_2MoO_6) and bismuth oxyhalide etc.

2.2.2 Photocatalysis mechanism of bismuth particles

Bismuth compound is stable photocatalytic activity which bismuth nanoparticles can inhibit microbial for more than 5 hours of irradiation. Dong F. et al. reported that bismuth nanoparticle sample after long irradiation time is identical to fresh sample therefore the results can be concluded that the Bi particles is excellent phase stability and performance stability. [17]

The equation of Bi-NPs photocatalysis mechanism can be written as follow:

$$\text{Bi-NPs} + h\nu \rightarrow h^+_{VB} + e^-_{CB} \quad \text{(a)}$$

$$h^+_{VB} + H_2O \rightarrow \bullet OH + H^+ \quad \text{(b)}$$

$$h^+_{VB} + OH^- \rightarrow \bullet OH_{ad} \quad \text{(c)}$$

$$e^-_{CB} + O_2 \rightarrow \bullet O_2^- \quad \text{(d)}$$

$$\bullet O_2^- \xrightarrow{2H^+} H_2O_2 \quad \text{(f)}$$

Visible light irradiation is absorbed in Bi-NPs. The decay of organic pollution and antimicrobial is carried out by through three mechanisms include the first mechanisms is the generation of electron-hole pairs (e^--h^+) after absorbed visible light or UV light irradiation which photon must equivalent or excess to band gap energy for photocatalytic degradation of toxic pollution. The band gap in semiconductor is the void of energy region between the valence band and conduction band. Electron excited from valence band to conduction band under UV light and visible light irradiation in Bi-NPs to generate photo-generated electron-hole pairs (e^--h^+) which are separated and migrated to photocatalyst surface. The redox reaction take place on photocatalyst surface to generate reactive oxidative species (ROSs). These photo-generated electrons are reacted with oxygen which is dissolved in solution adsorbed on photocatalysis surface to form superoxide anion radicals ($\bullet O_2^-$). In simultaneous, hole which is generated in valence band reacts with water (H_2O) to form hydroxyl radicals ($\bullet$OH). The superoxide anion radicals ($\bullet O_2^-$) and hydroxyl radicals ($\bullet$OH) which are highly active oxidant and high responsibility react to photodegrade pollutant molecule by decomposition of organic pollution and form carbon dioxide (CO_2), H_2O and other degradation products. [17-19] The mechanism of bismuth photocatalytic activities is shown in **Figure 4**.

The mentioned mechanism is ideal situation. Wang W. et al. are written about the fact of semiconductor mediated photocatalyst that the photocatalytic mechanism is mostly based on electronic potential of band structure in semiconductor material. The electronic potential of conduction band should be more negative than the redox potentials for formation of superoxide anion radicals. Photo-generated electrons are unstable and could not react with O_2 to form $\bullet O_2^-$ if electronic conduction band less negative than redox potentials. The electronic potential of valence band should be more positive than the redox potentials for formation of hydroxyl radicals. In addition, other factors affecting photocatalysis activities such as particle size, morphology of semiconductors and wavelength of light source. [19]

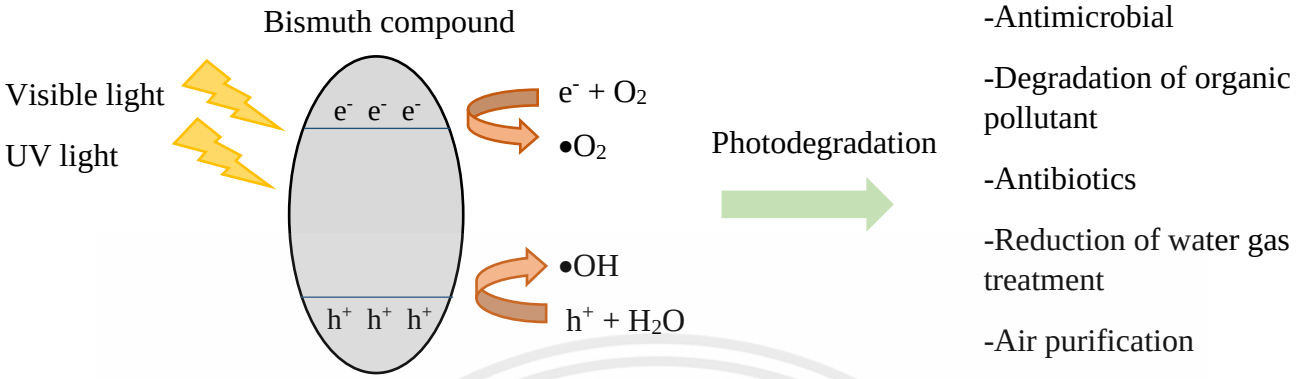

Figure 2.4 A schematic diagram showing the bismuth compound mechanism of photocatalytic oxidation process.

2.2.3 Bismuth oxide (Bi_2O_3) and Bismuth sulfide (Bi_2S_3)

Bismuth oxide (Bi_2O_3) is a common oxide semiconductor. The Bi_2O_3 has ban gap between 2.6 – 2.9 eV is widely used in chemical engineering and electronics. Bismuth sulfide (Bi_2S_3) has a narrow band gap between 1.3 – 1.7 eV. The Bi_2S_3-NPs is easily activated under visible light region for generating photoinduced electron and hole pairs. Bi_2S_3-NPs has the excellent photo-response because of lowest energy band gap of bismuth compound. During synthesis or photocatalytic activity, Bi_2S_3 may emit highly toxic fumes of oxides of sulfur. Bi_2O_3 is considered that non-toxic semiconductor material, however the effect of Bi_2O_3 in nanoscale on human heath for long period time can destroy cell. The bismuth based multi complex compound is safe than Bi_2O_3 and Bi_2S_3. [15,20]

2.2.4 Bismuth based multi-component oxide

Bismuth based multi-component oxide consists of bismuth titanate family, bismuth tungstate (Bi_2WO_6), Bismuth vanadate (Bi_2VO_4) and bismuth oxyiodide (BiOI) etc.

The family used of bismuth titanate for phtocatalysis are mainly $Bi_4Ti_3O_{12}$, $Bi_2Ti_2O_7$ and $Bi_{12}TiO_{20}$. The bismuth titanate has narrow ban gap between 2.5 – 2.8 eV. $Bi_4Ti_3O_{12}$ can be prepared via chemical composition method. The properties of $Bi_4Ti_3O_{12}$ exhibits photocatalytic activities to degrade methyl orange. [15]

Bismuth tungstate (Bi_2WO_6) is one of most attractive bismuth complex nanoparticle which has attractive properties such as high visible light, solar photocatalytic activity, high stability against photo-corrosion, and strong visible light absorption ability. The Bi_2WO_6 has a narrow ban gap between 2.6 – 2.7 eV. [16] The Bi_2WO_6 semiconductor presents many interesting prospects include piezoelectricity, ferroelectricity, non-linear dielectric susceptibility and excellent photocatalytic activity. The single phase of Bi_2WO_6 has highly effective in photocatalytic inactivation of *E-coli* is a negative gram bacterium under visible light irradiation. [19]

Bismuth vanadate (Bi_2VO_4) is one of visible light driven semiconductor for oxidation process which has mainly three crystal structures include tetragonal zircon, monoclinic and tetragonal scheelite structures. The Bi_2VO_4 has a narrow band gap of 2.4 eV for monoclinic structures which is high visible light absorption. [15,21] The color of Bi_2VO_4 is yellow pigment which used in paint industrial because of non-toxic pigment. The advantage of Bi_2VO_4 nanoparticles is non-toxic, environmentally friendly, high photocorrosion resistance and low cost.

Bismuth oxyiodide (BiOI) is categorized in the family of bismuth oxyhalides which is layered crystal structure in tetragonal matlockite form. [21] The BiOI has smallest band gap about 1.6 – 1.9 eV. The interested properties of BiOI are strong absorption under visible light irradiation, excellent photocatalytic activities under sun-light irradiation and BiOI photocatalytic activity towards up to 80 percent an antibiotic, ciprofloxacin degradation under indoor fluorescent light from lamp and 100 percent ciprofloxacin inactivation under visible light irradiation. [9] Furthermore, the crystal structure of BiOI is strongly other properties such as electronic, optic, oxidizing ability and high effective degradation of toxic pollution and environmental.

2.2.5 Application of bismuth nanoparticles

Bismuth particles (Bi) is widely used in waste and organic pollution treatment such as degradation of organic pollutants, degradation of textile dye, degradation of pharmaceutical products (antibiotics), water disinfection (bacteria removal), waste gas treatment (carbon dioxide reduction), water reduction in hydrogen production and air purification. The bismuth particles can inhibit bacteria growth at lower concentration than 1 mM. [16] Moreover, bismuth compounds are considered due to is one of the few heavy elements having special properties of good biocompatibility and non-toxicity for human body which can used in other nanotechnology including biomedical, photocatalyst, microelectronics, and sensor technology.

2.3 Literature review

Currently, bismuth compound is novel photocatalyst which has attracted much interest from many researchers because of its high visible light photocatalytic activities and non-toxicity. Yang et al. reported syntheses and application of bismuth complexes. There have 4 major methods, hydrothermal, solvothermal, microwave-based and routine solution syntheses. Hydrothermal synthesis yields single-crystal particle by operation at high temperature using aqueous solution and high vapor pressures, which is commonly carried out in Teflon-lined steel pressure autoclave. Solvothermal synthesis is commonly used due to the lower operating temperature than hydrothermal synthesis and obtains benefit of hydrothermal and sol-gel synthesis method. However, solvothermal synthesis takes longer period time. [22]

Most bismuth nanoparticles synthesis method will be operated in high temperature. Liu and Xu presented synthesis bismuth vanadate by facile and straightforward co-precipitation method at room temperature which provide monoclinic scheelite structure of $BiVO_4$ by mixing of $Bi(NO)_3.5H_2O$, NH_4VO_3, acetic acid and NaOH. Moreover, effect of different NaOH concentration for preparing $BiVO_4$ was studied that shows different photocatalytic dechlorination of *Rhodamine B* (*RhB*). [23] In addition, Adán et al. showed the synthesis and photocatalytic activities under UV-A and visible light of $BiVO_4$-NPs by reducing limitation of photocatalytic activities on bacteria cell surface via photocatalytic oxidation of methanol of $BiVO_4$. [24]

Besides photocatalytic of bismuth compound under visible light, BiOI also showed photocatalytic activities under fluorescent light. Yusoff et al. reported the synthesis of bismuth oxyiodide nanosphere and nanoplates as well as degradation of ciprofloxacin activities under visible light and fluorescent light. Crushed $Bi(NO)_3.5H_2O$ was mixed with polyethylene glycol (PEG400) and KI under room temperature for 20 min to form black paste. After that, product was washed several times with distilled water and absolute ethanal before dried in oven 80°C. The results showed narrow band gap energies of BiOI nanosphere and nanoplates (less than 2 eV) which indicate excellent photocatalysis activities under visible light of BiOI. In addition, these BiOI-NPs can be active under fluorescent light up to 80% degradation within 90 min. [9] To emphasized above article, Li et al. showed excellent methyl orange (MO) degradation of photocatalytic activities of BiOI

under 23W U-type compact fluorescent lamp as a light source. The photodegradation efficiency of BiOI under fluorescent lamp (around 425 nm) reach nearly 88%. Changing light source from fluorescent lamp to 500 W Xe-illuminator did not affect degradation efficiency. [8] Lee et al. showed the hydrothermal synthesis, characterization, photocatalytic activities of bismuth oxyiodide (BiOI) nanoparticle. BiOI nanoparticles were synthesized by mixing $Bi(NO)_3.5H_2O$ and HNO_3, followed by adjusting pH with NaOH to form white precipitate. Potassium iodide (KI) is added and stirred for 30 min before heating in autoclave at 130 – 280°C. The band gap energies of Bi-NPs were estimated to 1.86 – 3.1 eV. UV-vis absorption spectra represented steep shape at $\lambda > 400$ nm and strong absorption in visible light region. [25] Disadvantage of hydrothermal method was improved to reduce operating condition. Cai et al. synthesized BiOI nanoflowers at room temperature by mixing of $Bi(NO)_3.5H_2O$, polyvinylpyrrolidone (PVP), isopropyl alcohol and KI. The results show BiOI nanoflowers can degrade *Rhodamine B* (*RhB*) under visible light and higher photocatalytic activities than spherical. [26]

To confirmed the results of Cai et al., the photodegradation of phenol over nanostructured BiOI microsphere was compared with BiOI nanoplatelets, showed that the efficiency of photodegradation of BiOI microsphere is higher activity than BiOI nanoplatelets are 97% and 62%, respectively. Xiao et al. reported that three-dimensional (3D) nanostructure of BiOI microspheres are stable and can used to repletely and high photocatalytic performance. [27] BiOI formation in this study was prepared at room temperature in absolute ethanol to form BiOI microspheres and replacing ethanol with distilled water and without adjusting pH to form BiOI microplatelets.

CHAPTER III

RESEARCH METHODOLOGY

SPNR sheet was first dipped into an aqueous emulsion solution containing anionic surfactant (SDS), *tert*-butyl hydroperoxide (*t*-BuHP), methyl methacrylate (MMA) monomer and then dipped into bismuth(III) nitrate pentahydrate ($Bi(NO)_3.5H_2O$) solution. After that potassium iodide (KI) was added in solution. To initiate polymerization, the MMA-swollen rubber was then dipped into an alkaline solution of fructose and ferrous ion. In this work, the photodegradation properties of BiOI microparticles on modified SPNR sheets under UV light was studied.

3.1 Chemicals

1) Aluminum oxide (basic), Brockmann I grade, SIGMA-ALDRICH
2) Aluminum oxide (neutral), Brockmann I grade, SIGMA-ALDRICH
3) Ammonium iron (II) sulphate hexahydrate, AR grade, KEMAUS
4) Ammonia 30% for analysis, PanReac AppliChem ITW reagents
5) *tert*-Butyl hydroperoxide (70%) (*t*-BuHP), SIGMA-ALDRICH
6) D- (-)-Fructose, ≥99%, SIGMA-ALDRICH
7) Deionized water
8) Methanol, commercial grade
9) Methyl methacrylate (MMA), 99%, ACROS ORGANICS
10) Sodium dodecyl sulphate (SDS), ≥98.5%, SIGMA-ALDRICH
11) Bismuth (III) nitrate pentahydrate ($Bi(NO)_3.5H_2O$), AR grade, KEMAUS
12) Potassium iodide (KI), AR grade, UNIVAR
13) Isopropyl alcohol (C_3H_8O), commercial grade
14) Sodium hydroxide (NaOH), commercial grade
15) Stearic acid, commercial grade
16) Sulphur Prevulcanized Natural Rubber (SPNR) latex, Thai Rubber Latex Group Public Company Limited.

3.2 Apparatus

1) Aluminum foil
2) Aluminum sieves (250 mesh)
3) Amber glass bottle
4) Analytical balance
5) Beaker
6) Mortar and pestle
7) Centrifugal tubes
8) Circulating Baths with MX Temperature Controller, Polyscience
9) Cotton
10) Filter paper
11) Glass column
12) Jacket reactor (300 ml and 600 ml)
13) Magnetic bar
14) Magnetic stirrer
15) Para film
16) Plastic bag
17) Plastic film
18) pH paper
19) Oven
20) Rubber gloves
21) Silica gel
22) Sonicating bath
23) Spatula
24) Home built spin coater
25) Stainless steel scissors

3.3 Experimental

3.3.1 Preparation of SPNR sheet

1) Pour 150 ml SPNR latex through 250-mesh sieve 3 times to filter rubber clumb and dust from SPNR latex. Then scoop small bubbles out from the latex.
2) Gently, pour filtered SPNR latex to a glass plate.
3) Dry SPNR latex at 60°C overnight.

Figure 3.1 Images of SPNR sheet

3.3.2 Cleaning SPNR sheet

1) Cut SPNR sheet into 1.5x4 cm^2.
2) Put SPNR strip in centrifugal tubes and pour methanol into the beaker.
3) Sonicate the rubber strip in the beaker for 15 minutes.
4) Drain methanol and repeat by changing methanol to deionized water.
5) Store cleaned SPNR strip in box containing silica gel.

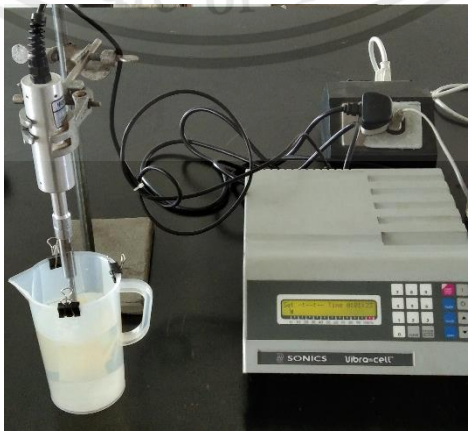

Figure 3.2 Images of cleaning step

3.3.3 Purification of MMA monomer

1) Insert cotton into the tip of glass column.
2) Add neutral aluminum oxide and basic aluminum oxide into the column, respectively.
3) Wrap the column with aluminum foil and pack the ice pads to cool the system.
4) Pour non-purified MMA monomer into the prepared column. Collect the purified MMA monomer and store in an amber glass bottle at 4°C.

Figure 3.3 Images of MMA purification

3.3.4 Formation of BiOI microparticles and PMMA-modified SPNR sheet

1) Prepare an aqueous emulsion solution containing purified MMA monomer (62.5 g), 2% aqueous solution of SDS (191.2 g), 70% *t*-BuHP (6.7 g) and stir at 700 rpm for 20 minutes.
2) Dip cleaned rubber strip in the emulsion solution in step 1 and stir at 700 rpm for 20 minutes.
3) Prepare 1%wt of bismuth (III) nitrate pentahydrate in deionized water and stir until solution change to turbid white solution (homogenous solution).
4) Dip MMA-swollen rubber strip into prepared bismuth solution and stir at 700 rpm at various dipping times.

5) Prepare 3%wt of potassium iodide in deionized water.
6) Pour prepared potassium iodide solution into bismuth solution in step 4) and continuously stir for 40 minutes.
7) Dip BiOI/MMA-swollen SPNR strip into deionized water and stir at 400 rpm for 5 minutes to clean the residue MMA emulsion and excess BiOI particles on rubber strip.
8) Prepare 150 ml mixture of an aqueous solution of 2% fructose and 10 ppm ferrous ion at pH 10 in jacket reactor and heat to 60˚C.
9) Dip cleaned MMA-swollen with BiOI rubber in the alkaline aqueous solution at 60˚C for 6 h.
10) Rinse surface-modified rubber sheet with deionized water.
11) Store samples (BiOI/PMMA-modified SPNR sheets) in the box containing silica gel.

3.3.6 Photocatalytic activities test

1) Cut prepared BiOI/PMMA-modified SPNR sheets into 1.5x1.5 cm^2
2) Prepare 6%wt stearic acid in isopropyl alcohol.
3) Coat stearic acid on BiOI/PMMA-modified SPNR sheets using spin-coater at 400 rpm
4) Dry stearic acid which coated on BiOI/PMMA-modified SPNR sheets in room temperature
5) Irradiate UV-A light region (T5, 8 watts), λ = 345-400 nanometer, on prepared BiOI/PMMA-modified SPNR sheets in step 4) for 24 hours. Setting distance between light and sample is 15 cm.

3.3.5 Characterization

1) The surface morphologies of SPNR sheets and modified SPNR sheets which was coated with thin layer of platinum and palladium for 1.5 minutes, and elemental analysis using scanning electron microscopy with energy dispersive X-ray spectroscopy (SEM/EDX) (EVO® HD from Carl Zeiss)

and field emission scanning electron microscopes (FE-SEM) (HITACHI SU-8010).

2) The structure of BiOI powder and BiOI particles on SPNR and modified SPNR was characterized using X-ray diffractometer (SHIMADZU XRD-6100).
3) Thermogravimetric measurements were carried out to determine percentage of residue on modified SPNR using thermogravimetric analyzer (Perkin Elmer-Pyris 1)
4) The surface functional groups of BiOI and degradation of BiOI/PMMA-modified SPNR sheets were investigated by using Fourier-transform infrared spectroscopy (FT-IR) (SHIMADZU IRP restige-21).

CHAPTER IV
RESULTS AND DISCUSSION

This work aims to synthesize bismuth oxyiodide (BiOI) microparticles to modify the surface of SPNR sheets by installing BiOI and PMMA on rubber sheets. Effect of pH, concentration of potassium iodide (KI) and dipping time of bismuth(III) nitrate pentahydrate in aqueous solution on morphology and content of BiOI on SPNR sheets were investigated by scanning electron microscopy with energy dispersive X-ray spectroscopy (SEM/EDX). The structure of prepared BiOI/PMMA on SPNR sheets were characterized by the X-Ray diffractometer (XRD), thermogravimetric analyzer (TGA), and fourier-transform infrared spectroscopy (FTIR). The photodegradation activities on BiOI/PMMA on SPNR sheets under UV-visible light were analyzed using FTIR technique.

4.1 Formation of BiOI on SPNR sheets (1%wt of $Bi(NO_3)_3.5H_2O$)

4.1.1 Effect of concentration of KI

Figure 4.1 shows SEM images of BiOI-coated SPNR sheets, prepared by dipping SPNR sheets in 1%wt $Bi(NO_3)_3.5H_2O$ solution, prior to the addition of various concentration of KI solution. Compared to bare SPNR sheets in **Figure 4.1(a)**, the amount of BiOI formed on SPNR increased with increasing KI concentrations, which agreed with EDX analysis **(Table 1)**. The amount of KI also affects the size and dispersion of BiOI microparticles at 3%wt KI showed the largest particle and highest coverage as showed in **Figure 4.1 (d). Figure 4.2** shows higher resolution of $Bi(NO_3)_3.5H_2O$ solution with 3% KI. The uniform micron-sized flakes were formed on SPNR sheet.

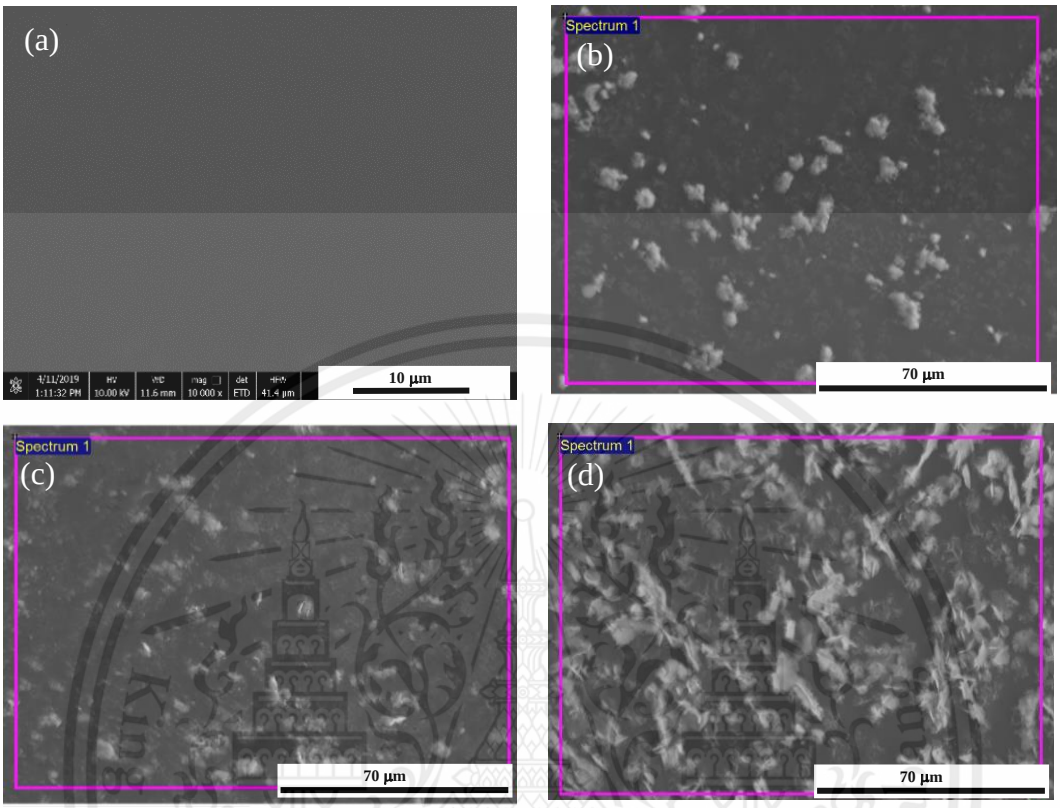

Figure 4.1 SEM micrographs of (a) bare SPNR sheet and BiOI-coated on SPNR sheets using (b) 1%wt, (c) 2%wt and (d) 3%wt of KI

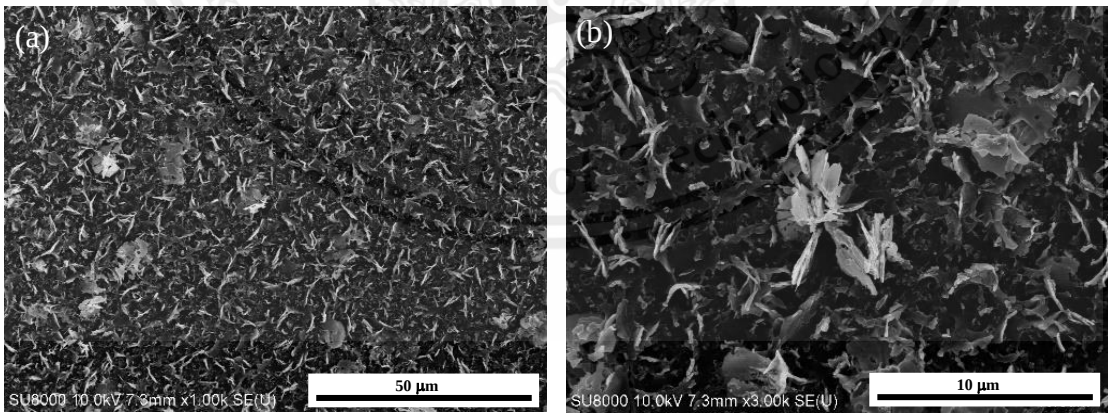

Figure 4.2 FE-SEM micrographs of BiOI-coated on SPNR sheets

Table 4.1 The amount of BiOI on SPNR sheets at various KI concentration

%KI	%Bi	%I
0 (SPNR)	0	0
1	1.58	1.20
2	1.89	1.39
3	8.24	6.03

% Bi and %I: the weight percentage of bismuth and iodide of selected-area using EDX analysis

In parallel, direct absorption of preformed BiOI particles was studied. $Bi(NO_3)_3.5H_2O$ solution was mixed with various concentration of KI until the brick-red solution, an indication of BiOI particles, was formed. Then, SPNR sheets were dipped in the suspension of BiOI particles for 30 minutes. SEM image in **Figure 4.3 (a)-(c)** showed small amount of BiOI particles adsorbed on SPNR sheets, compared to the previous study (**Fig. 4.1 (a)**). These results agree with the amount of Bi and I from EDX study in **Table 4.2**. Direct formation of BiOI particles on SPNR sheets provide the larger yield and surface coverage. This might be due to the presence of non-rubber component on rubber sheets. [28] Thus, direct formation of BiOI particles using 3%wt KI was chosen for the next study.

Table 4.2 The amount of Bi and I on SPNR sheets dipped into mixing BiOI solution at various KI concentration

%KI	%Bi	%I
0 (SPNR)	0	0
1	0.6	0.83
2	2.3	1.9
3	3.57	3.16

% Bi and %I: the weight percentage of bismuth and iodide of selected-area using EDX analysis

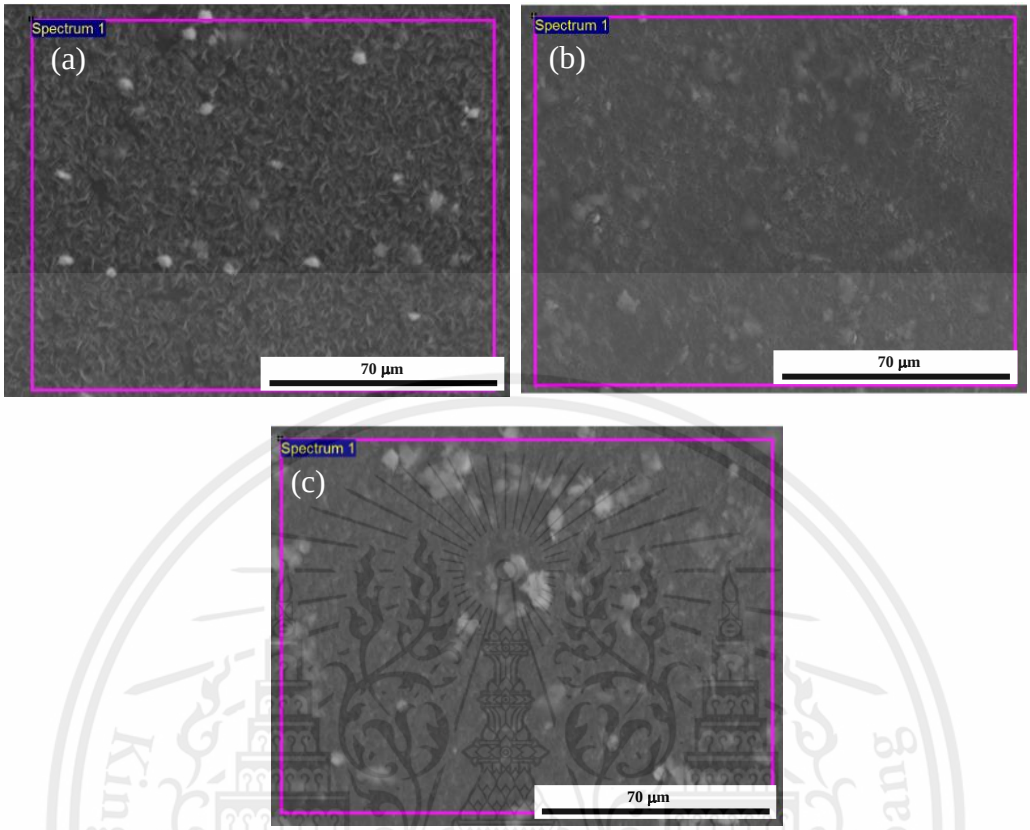

Figure 4.3 SEM micrographs of BiOI-coated on SPNR sheets by mixing (a) 1%wt KI, (b) 2%wt KI, and (c) 3%wt KI in 1%wt $Bi(NO_3)_3.5H_2O$ solution before dipping SPNR sheets

4.1.2 Effect of pH

Besides concentration of KI, pH of reaction solution also affects the morphology of BiOI particles. 4 pH were investigated, i.e., 2.3, 3, 4 and 5. When mixing $Bi(NO_3)_3.5H_2O$ and KI, its pH is around 2.3 and color of BiOI powder is brick-red. Increasing pH of solution changed the color of resulting powder from brick-red (pH = 2.3) to reddish orange (pH ≈ 3-4) and light orange at pH 5 as shown in **Figure 4.4.**

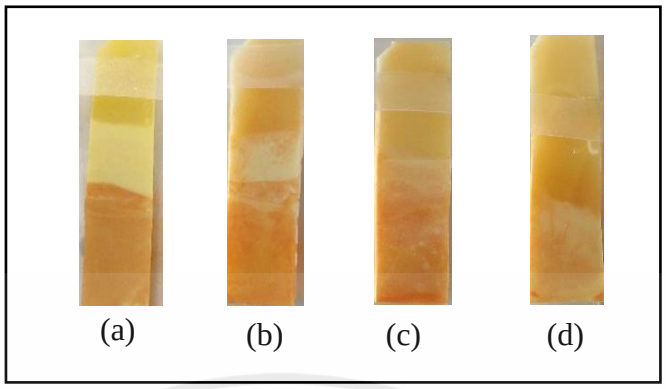

Figure 4.4 Images of BiOI-coated on SPNR sheets prepared in BiOI solution at (a) pH 2.3, (b) pH 3, (c) pH 4 and (d) pH 5.

EDX analysis in **Figure 4.6** presented that percentage of bismuth and iodide increases when increasing pH from pH 2.3 to pH 3 then decreases. **Figure 4.5** shows SEM images of BiOI-modified SPNR sheets. It is clear that morphology of BiOI changes from flake-like at pH 2.3 to particles-like structure at higher pH (3-5). The flake-like microstructure obtained lower lamella thickness. These results indicate that pH of reaction solution affect both morphology and adsorption of BiOI on SPNR sheets. From these studies, pH = 2.3 was selected for further studies due to the desired structure of BiOI.

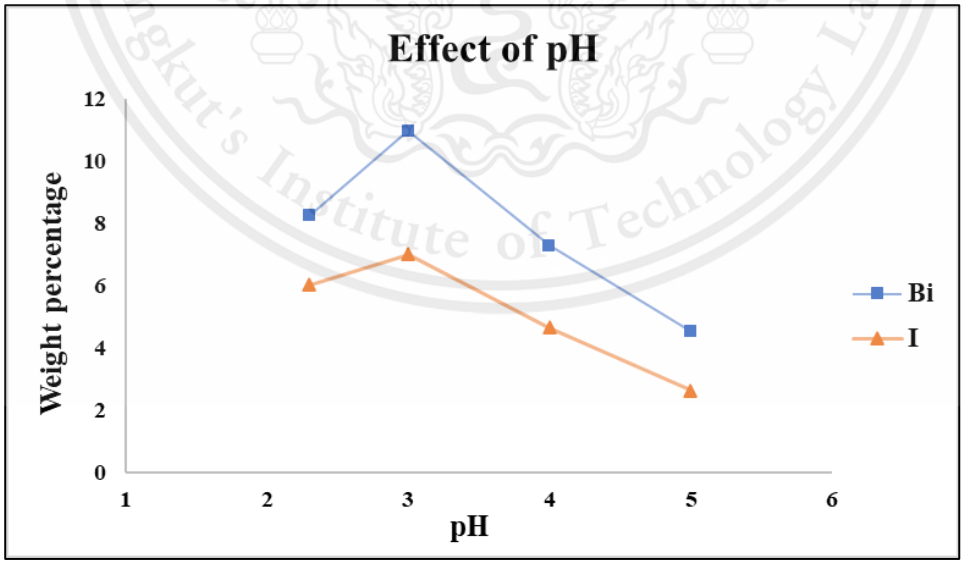

Figure 4.5 Images of BiOI-coated on SPNR sheets at (a) pH 2.3, (b) pH 3, (c) pH 4 and (d) pH 5 of BiOI solution

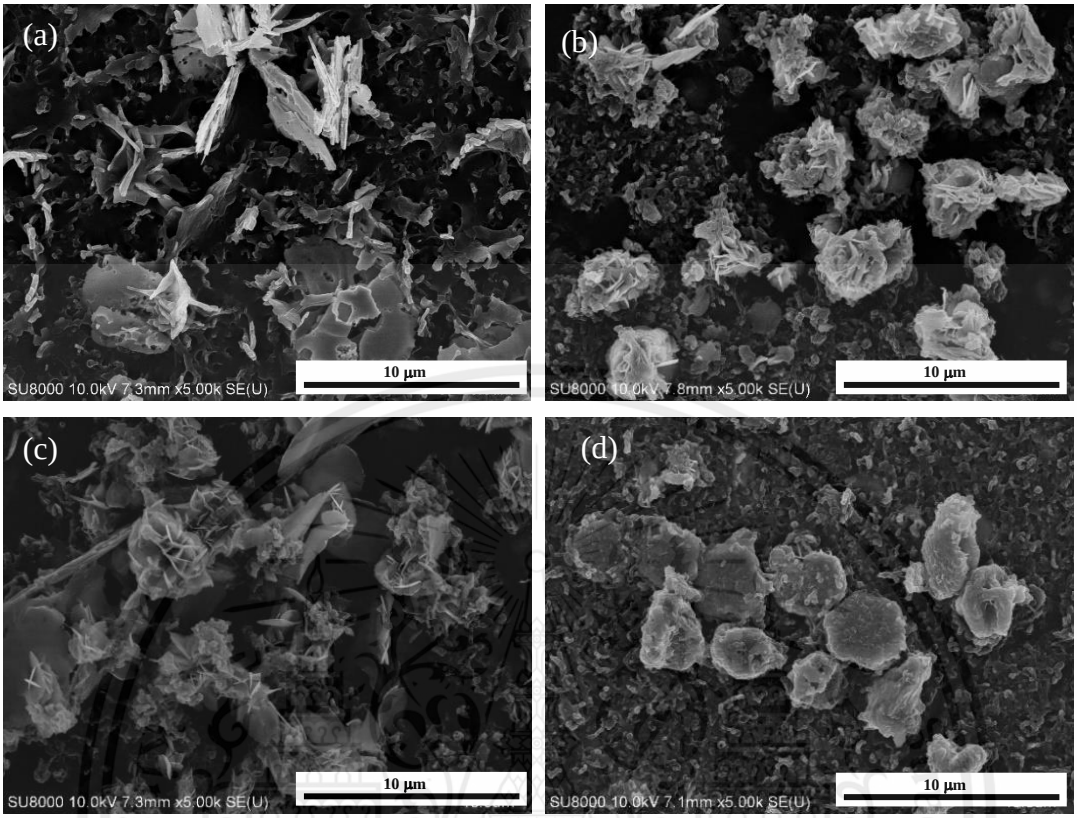

Figure 4.6 SEM micrographs of BiOI-coated on SPNR sheets at (a) pH 2.3, (b) pH 3, (c) pH 4 and (d) pH 5 of BiOI solution

4.2 Formation of BiOI microflowers/PMMA on SPNR sheets.

Formation of BiOI particles on MMA-swollen SPNR sheets due to low glass transition temperature (T_g) of natural rubber. Performance of functional particles (e.g. silver (Ag) particles) on the surface of rubber film decreases because Ag particles sink into the soft rubber matrix. [28] Enhance rigidity at the rubber surface is then necessary. In this study, PMMA layer was prepared at the SPNR/BiOI interface. SPNR was swollen with MMA emulsion, containing *t*-BuHP, and SDS. Then, MMA swollen rubber was dipped into $Bi(NO_3)_3.5H_2O$ solution to form BiOI powder as discussed. MMA in rubber was converted to PMMA, after polymerization in ferrous ion/fructose solution at 60˚C for 6 hours.

Figure 4.7 shows XRD patterns of BiOI powder BiOI-coated SPNR and BiOI-coated SPNR/PMMA, respectively. XRD pattern of BiOI powder prepared by using 1% $Bi(NO_3)_3.5H_2O$ and 3% KI at pH 2.3 has strong diffraction peaks at 29.55, 33.13, 45.59 and 55.19, suggesting the formation of pure tetragonal phase of BiOI. It is also confirmed by JCPDS (card no. 00-010-0445) in **Appendix A.2.** Though lower intensity, some diffraction peaks (as indicated) of tetragonal BiOI phase appeared on diffraction pattern of BiOI-coated SPNR and BiOI coated SPNR/PMMA. The lower resolution is due to the amorphous rubber. These results imply that BiOI powder and BiOI on solid substrates have similar phase.

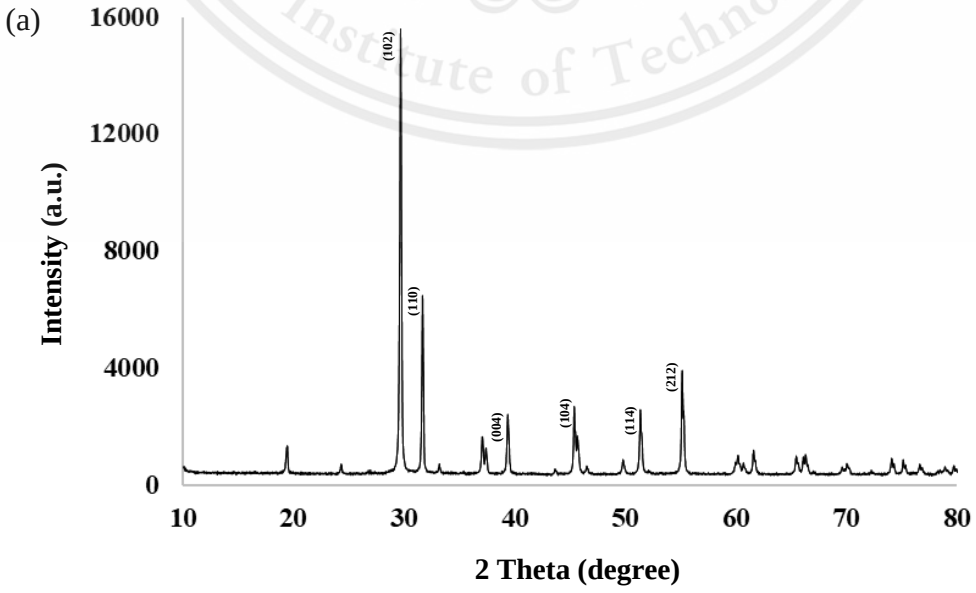

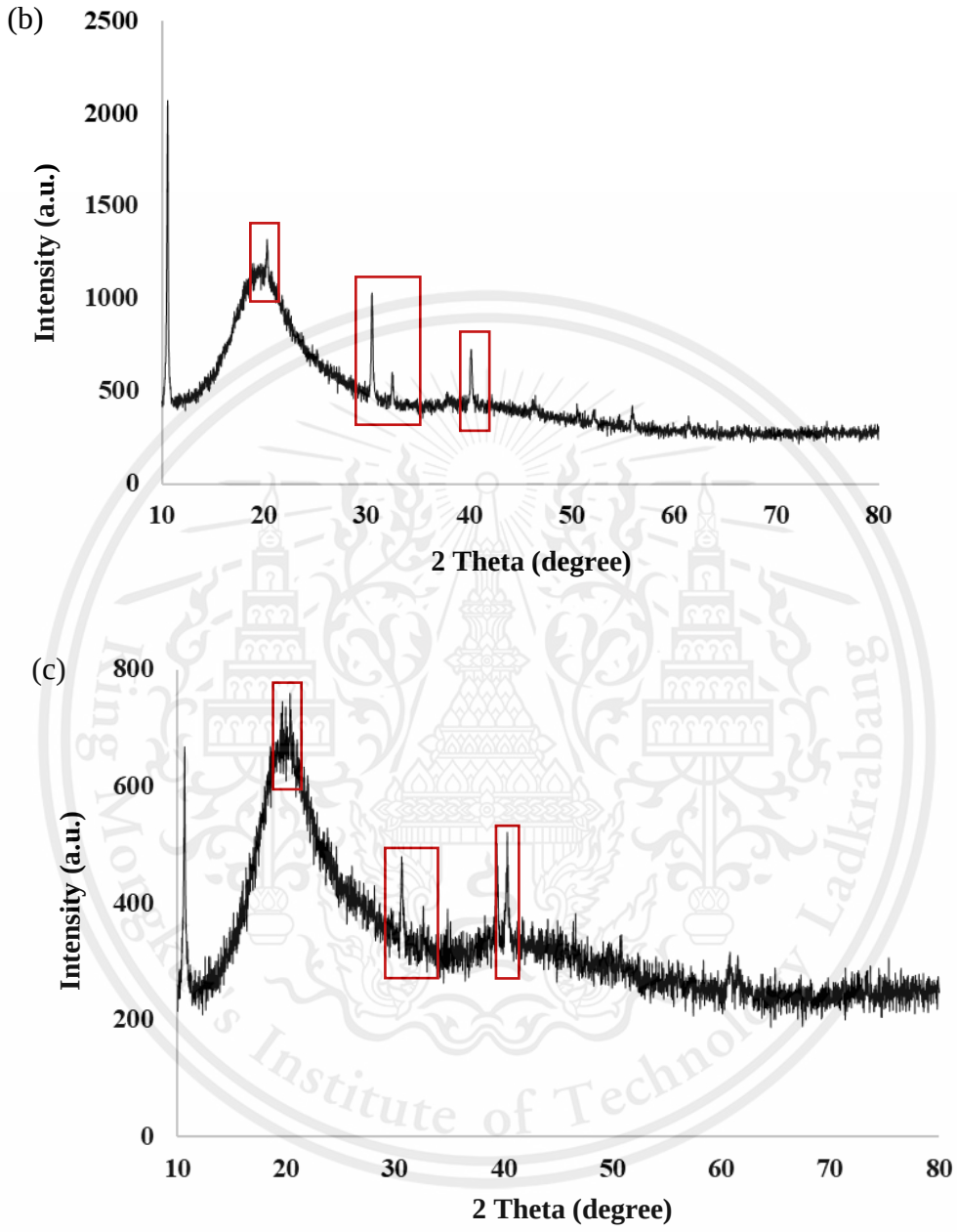

Figure 4.7 XRD patterns of (a) BiOI microparticles, (b) BiOI-coated SPNR sheets and (c) BiOI/PMMA-modified SPNR sheets

To enhance the amount of BiOI, MMA-swollen SPNR sheet was dipped in $Bi(NO_3)_3.5H_2O$ solution at various times. **Table 4.3** shows %residue from TGA measurement and %Bi as well as %I from EDX analysis **(Appendix A.1)**. %Residue increases with dipping time from 3.94 to 4.51 except at dipping time of 30 and 60 minutes. While %Bi and %I are directly proportional to dipping time.

Table 4.3 Percentage of residue, bismuth and iodide of BiOI coated SPNR/PMMA at various dipping times of $Bi(NO_3)_3.5H_2O$ solution

Dipping time in $Bi(NO_3)_3.5H_2O$ (min)	**% Residue**	**% Bi**	**% I**
10	3.94	0.85	0.4
20	5.04	1	0.5
30	4.33	11.84	6.19
40	5.20	16.93	9.19
50	5.33	17.19	9.11
60	4.51	45.84	25.5

% Bi and %I: the weight percentage of bismuth and iodide of selected-area using EDX analysis

FT-IR spectra as shown in **Figure 4.8** was used to determine surface functional groups and confirm the formation of BiOI particles on modified SPNR. The absorption peak at around 500 cm^{-1} can be assigned as Bi-O stretching vibration in BiOI. [9] The absorption band of PMMA observed at 1732, 1442 and 3035-2850 cm^{-1} are attributed to the presence of C=O stretching vibration, the bending of C-H and C-H stretching vibration.

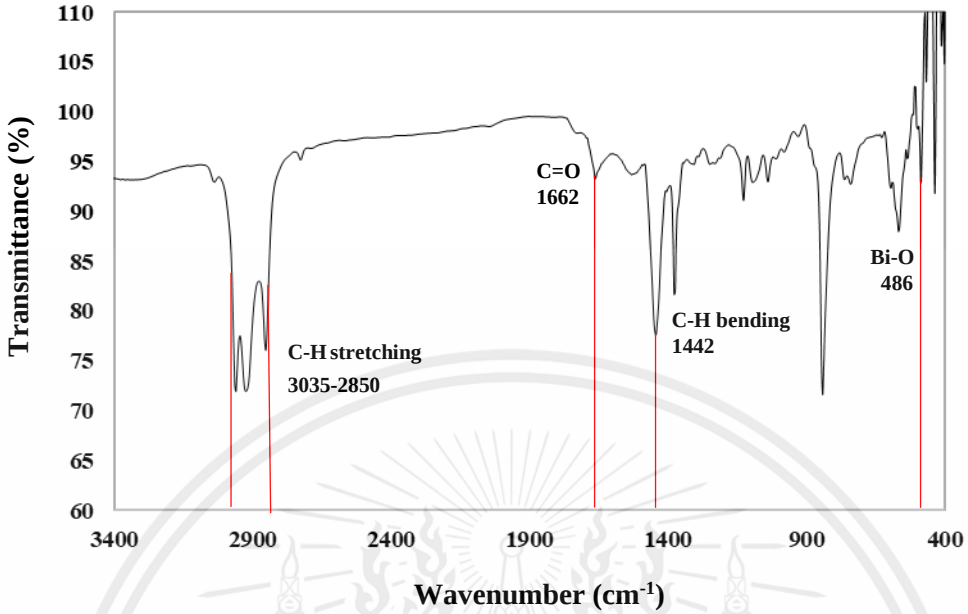

Figure 4.8 FT-IR spectra of BiOI/PMMA-modified SPNR sheets

Figure 4.9 as shows FE-SEM image of PMMA-modified SPNR presents limb or branch structure of PMMA formed and protruded out on SPNR substrate. SEM image of BiOI/PMMA-modified SPNR prepared at various dipping times in **Figure 4.10 (a)-(f)** reveal that the formation of BiOI increase with increasing dipping time, similar to TGA and EDX analysis. Size and structure of flake become larger with dipping time. Jamil et al. reported that these flaky morphologies provided higher photocatalytic performance. [27,29]

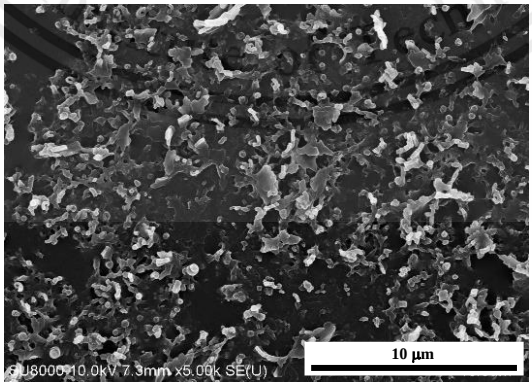

Figure 4.9 FE-SEM micrographs of PMMA-modified SPNR sheets

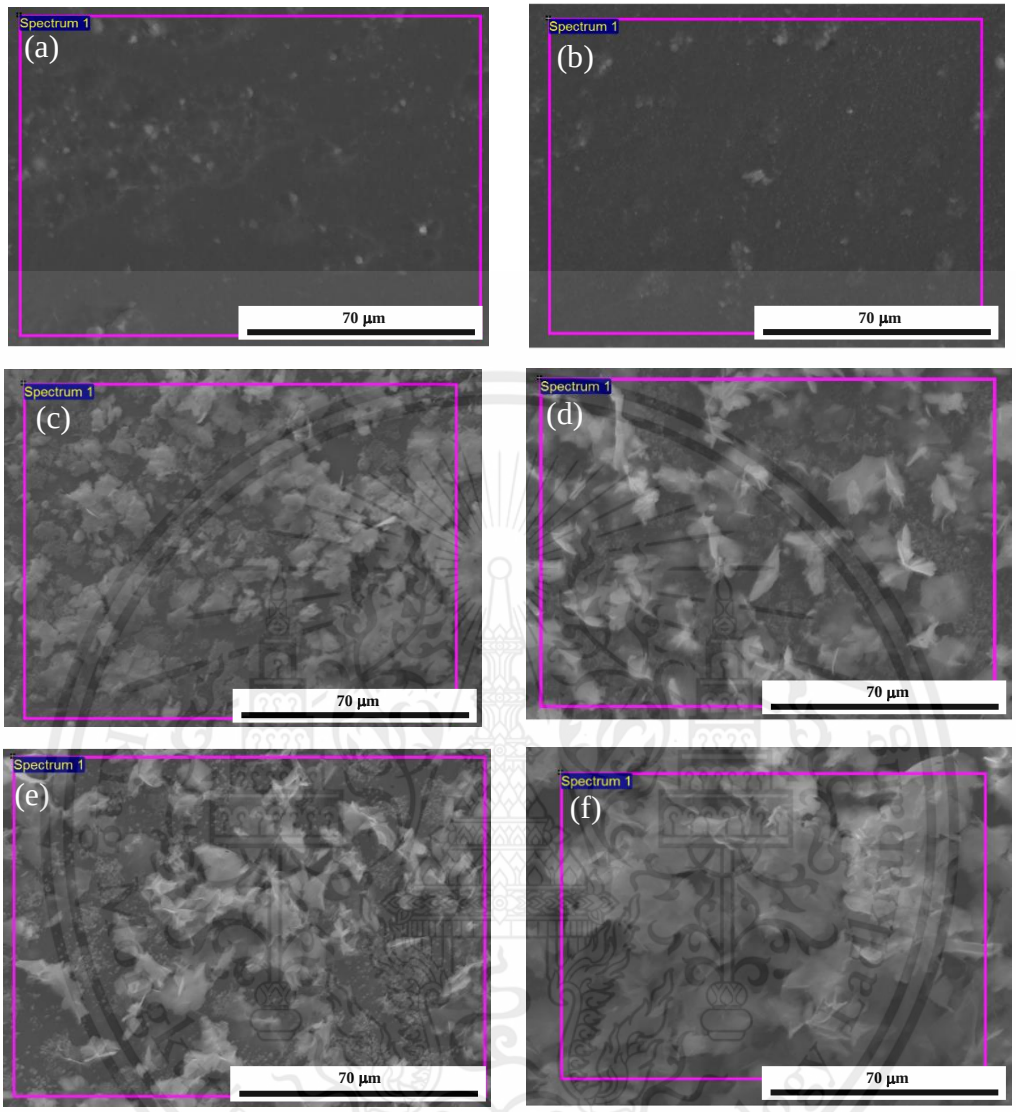

Figure 4.10 SEM micrographs of BiOI/PMMA-modified SPNR sheets by vary dipping time of $Bi(NO_3)_3.5H_2O$ in DI water at (a) 10, (b) 20, (c) 30, (d) 40, (e) 50 and (f) 60 minutes

The dipping time of $Bi(NO_3)_3.5H_2O$ solution was expected to affect the amount of bismuth and iodide on SPNR sheets. At 10 and 20 minutes of dipping time, small BiOI microplates were formed (**Figure 4.8 (a)-(b)**), At 30 minutes of dipping time, BiOI particles has been initiate to form nanoplates on SPNR. At 40, 50 and 60 minutes of dipping times, the 3D hierarchical BiOI nanoflowers were constructed from nanoplates. BiOI/PMMA-modified SPNR sheets at 60 minutes intensively appear the lowest thickness nanoplates of BiOI as shown in **Figure 4.11**. Lui and Xiao reported that 3D-hierarchal flower like microparticles has higher photocatalytic performance than other form of BiOI

particles, which results from large specific area and low lamella thickness [27,28]. Thus, BiOI/PMMA-modified SPNR sheets prepared at 60 minutes of dipping time was chosen to study photocatalytic activities in **Section 4.5.**

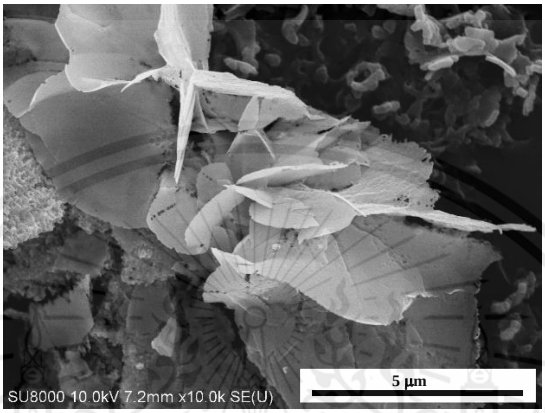

Figure 4.11 FE-SEM micrographs of BiOI/PMMA-modified SPNR sheets at 60 minutes of dipping time

4.3 Photocatalytic activity of BiOI/PMMA-modified SPNR

To investigate the photocatalytic performance of BiOI/PMMA-modified SPNR prepared at 60 minutes of dipping time. Stearic acid (SA), a model organic, was coated on the modified rubber before UV irradiation at wavelength of 345 - 400 nm. The degradation of SA was studied using FT-IR technique. The FT-IR spectrum of PMMA-modified SPNR and BiOI/PMMA-modified SPNR in **Figure 4.12** and **4.13 (a)** are similar, except the Bi-O bending at 447 cm^{-1}. **Figure 4.13 (b)** shows the FT-IR spectra of SA-coated BiOI/PMMA-modified SPNR before UV irradiation. The 2 additional peaks of SA at 1735 and 1246 cm^{-1} of C=O stretching and C-O bending, were observed. After being irradiated for 24 hours, the intensity of these 2 peaks become significantly low, suggesting the degradation of SA. Compared to FT-IR spectrum at longer irradiation time (45 and 54 hours) in **Figure 4.13 (c)-(e)** insignificant difference was observed.

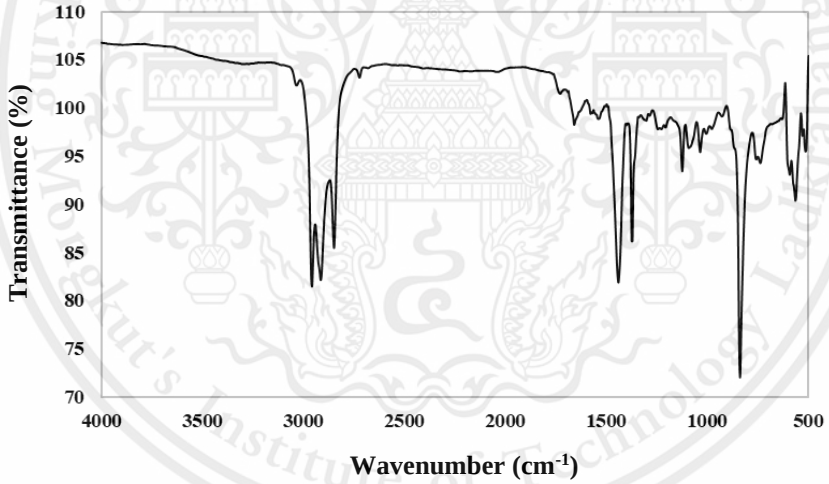

Figure 4.12 FT-IR spectra of PMMA-modified SPNR sheets

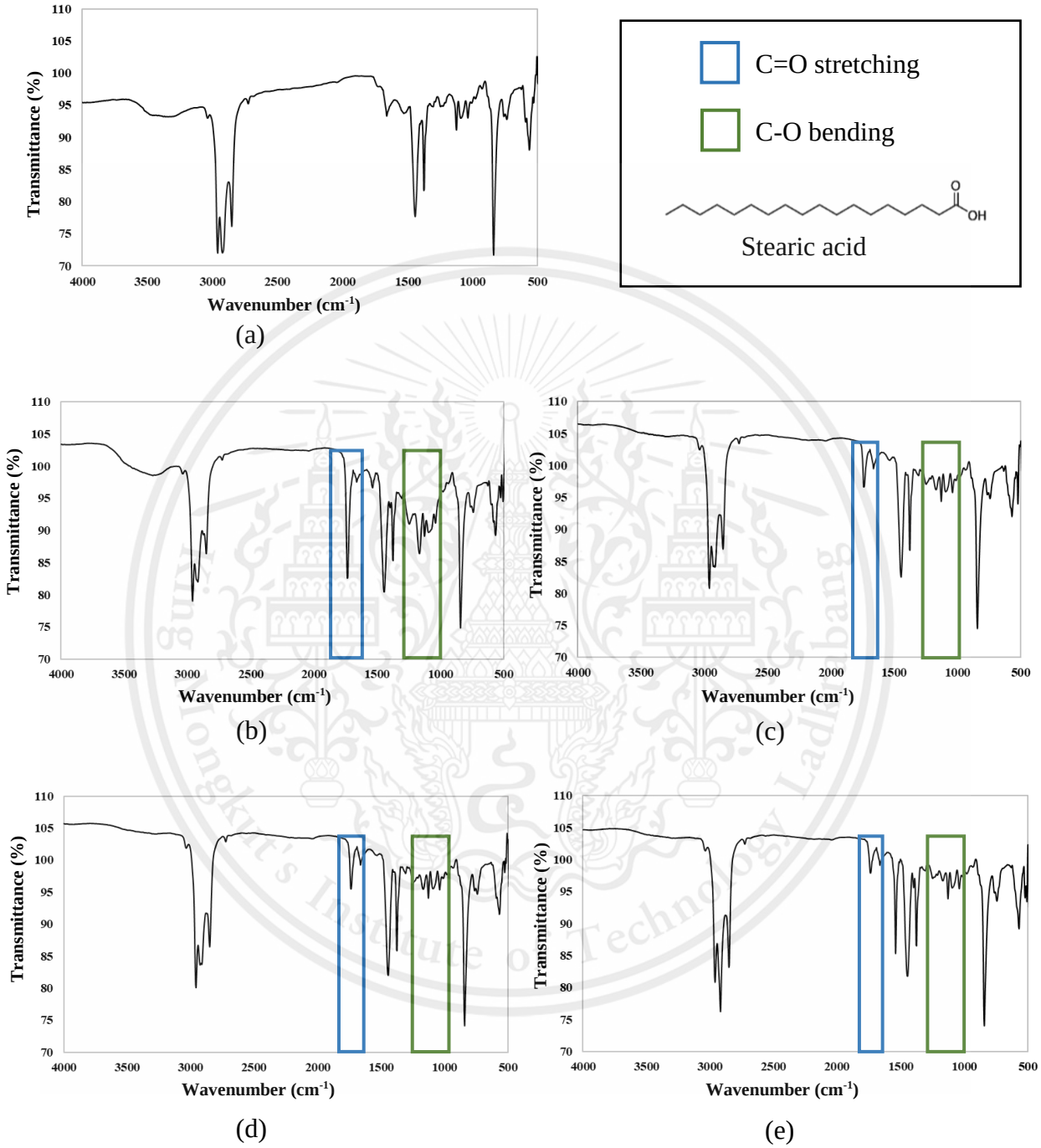

Figure 4.13 FT-IR spectra of (a) BiOI/PMMA-modified SPNR prepared at 60 minutes of dipping time, (b) BiOI/PMMA-modified SPNR with SA, (c) BiOI/PMMA-modified SPNR with SA under UV light irradiation for 24, (d) 45 and (e) 54 hours

CHAPTER V

CONCLUSIONS

In summary, the surface modification of sulfur pre-vulcanized natural rubber (SPNR) sheets has been successfully modified with PMMA and BiOI microparticles. SEM observation of prepared samples showed that the 3D-structure of flower-like BiOI microparticles was formed on PMMA after polymerization reaction at 60 minutes of dipping time. KI concentration and pH are important factors which affect morphologies and amount of BiOI on substrate. XRD and FT-IR analysis of BiOI/PMMA-modified SPNR suggested the presence of tetragonal phase of BiOI particles on SPNR sheets. Under UV light irradiation, the 3D structure of BiOI flower like microplates/PMMA-modified on SPNR sheets are able to effectively degrade stearic acid.

REFERENCES

(1) W. Anancharungsuk, W. Taweepreda, S. Wirasate, R. Thonggoom, and P. Tangboriboonrat, “Reduction of surface friction of natural rubber film coated with PMMA particle: Effect of particle size,” Journal of Applied Polymer Science, vol. 115, no. 6, pp. 3680–3686, Mar. 2010.

(2) W. Anancharungsuk, S. Tanpantree, A. Sruanganurak, and P. Tangboriboonrat, “Surface modification of natural rubber film by UV-induced graft copolymerization with methyl methacrylate,” Journal of Applied Polymer Science, vol. 104, no. 4, pp. 2270–2276, 2007.

(3) A. Sruanganurak, K. Sanguansap, and P. Tangboriboonrat, “Layer-by-layer assembled nanoparticles: A novel method for surface modification of natural rubber latex film,” Colloids and Surfaces A: Physicochemical and Engineering Aspects, vol. 289, no. 1–3, pp. 110–117, Oct. 2006.

(4) W. Anancharungsuk, D. Polpanich, K. Jangpatarapongsa, and P. Tangboriboonrat, “In vitro cytotoxicity evaluation of natural rubber latex film surface coated with PMMA nanoparticles,” Colloids and Surfaces B: Biointerfaces, vol. 78, no. 2, pp. 328–333, Jul. 2010.

(5) N. Kanjanathaworn, C. Kaewsaneha, D. Polpanich, K. Jangpatarapongsa, and P. Tangboriboonrat, “Composite Nanoparticles on the Natural Rubber Latex Glove for Reduction of Surface Friction and Cytotoxicity,” Polymers and Polymer Composites, vol. 20, no. 1–2, pp. 197–200, Feb. 2012.

(6) J. Wongpreecha, D. Polpanich, T. Suteewong, C. Kaewsaneha, and P. Tangboriboonrat, “One-pot, large-scale green synthesis of silver nanoparticles-chitosan with enhanced antibacterial activity and low cytotoxicity,” Carbohydrate Polymers, vol. 199, pp. 641–648, Nov. 2018.

(7) T. Suteewong, J. Wongpreecha, D. Polpanich, K. Jangpatarapongsa, C. Kaewsaneha, and P. Tangboriboonrat, “PMMA particles coated with chitosan-silver nanoparticles as a dual antibacterial modifier for natural rubber latex films,” Colloids and Surfaces B: Biointerfaces, vol. 174, pp. 544–552, Feb. 2019.

(8) Y. Li, J. Wang, H. Yao, L. Dang, and Z. Li, “Efficient decomposition of organic compounds and reaction mechanism with BiOI photocatalyst under visible light

irradiation," Journal of Molecular Catalysis A: Chemical, vol. 334, no. 1–2, pp. 116–122, Jan. 2011.

(9) M. A. M. Yusoff, S. S. Imam, I. Shah, and R. Adnan, "Photocatalytic activity of bismuth oxyiodide nanospheres and nanoplates in the degradation of ciprofloxacin under visible light," Materials Research Express, vol. 6, no. 8, p. 0850g5, Jun. 2019.

(10) T. Saison, N. Chemin, C. Chanéac, O. Durupthy, L. Mariey, F. Maugé, V. Brezová, and J.-P. Jolivet, "New Insights Into BiVO4 Properties as Visible Light Photocatalyst," The Journal of Physical Chemistry C, vol. 119, no. 23, pp. 12967–12977, Jun. 2015.

(11) C. M. Roland, "Interpenetrating Polymer Networks (IPN): Structure and Mechanical Behavior," Encyclopedia of Polymeric Nanomaterials, pp. 1–9, 2013.

(12) A. P. Mathew, "Interpenetrating Polymer Networks: Processing, Properties and Applications," Advances in Elastomers I, pp. 283–301, 2013.

(13) B. Briscoe, Fundamentals of Polymer Wear. 1985, 3, 647–651.

(14) Shivashankar, M.; Mandal, "Review on Interpenetrating Polymer Network." *Int. J. Pharm. Pharm. Sci.* 2012, *4* (SUPPL. 5), 1–7.

(15) R. He, S. Cao, P. Zhou, and J. Yu, "Recent advances in visible light Bi-based photocatalysts," Chinese Journal of Catalysis, vol. 35, no. 7, pp. 989–1007, Jul. 2014.

(16) Claudio C.-R., Chellam S. "Bismuth Nanoparticles: Antimicrobials of Broad-Spectrum, Low Cost and Safety", Chapter 17 in Nanomedicine. Nanomedicine 2014, 1, 430–438.

(17) F. Dong, T. Xiong, Y. Sun, Z. Zhao, Y. Zhou, X. Feng, and Z. Wu, "A semimetal bismuth element as a direct plasmonic photocatalyst," Chem. Commun., vol. 50, no. 72, pp. 10386–10389, 2014.

(18) C. Regmi, B. Joshi, S. K. Ray, G. Gyawali, and R. P. Pandey, "Understanding Mechanism of Photocatalytic Microbial Decontamination of Environmental Wastewater," Frontiers in Chemistry, vol. 6, Feb. 2018.

(19) W. Wang, G. Huang, J. C. Yu, and P. K. Wong, "Advances in photocatalytic disinfection of bacteria: Development of photocatalysts and mechanisms," Journal of Environmental Sciences, vol. 34, pp. 232–247, Aug. 2015.

(20) M. Abudayyak, E. Öztaş, M. Arici, and G. Özhan, “Investigation of the toxicity of bismuth oxide nanoparticles in various cell lines,” Chemosphere, vol. 169, pp. 117–123, Feb. 2017.

(21) W. W. Anku, S. O. B. Oppong, and P. P. Govender, “Bismuth-Based Nanoparticles as Photocatalytic Materials,” Bismuth - Advanced Applications and Defects Characterization, Jun. 2018.

(22) Y. Yang, R. Ouyang, L. Xu, N. Guo, W. Li, K. Feng, L. Ouyang, Z. Yang, S. Zhou, and Y. Miao, “Review: Bismuth complexes: synthesis and applications in biomedicine,” Journal of Coordination Chemistry, vol. 68, no. 3, pp. 379–397, Jan. 2015.

(23) C. J. Liu and Y. H. Xu, “Synthesis, Characterization and Photocatalytic Activities of Bismuth Vanadate by Facile Co-Precipitation Method,” Advanced Materials Research, vol. 148–149, pp. 1469–1472, Oct. 2010.

(24) C. Adán, J. Marugán, S. Obregón, and G. Colón, “Photocatalytic activity of bismuth vanadates under UV-A and visible light irradiation: Inactivation of Escherichia coli vs oxidation of methanol,” Catalysis Today, vol. 240, pp. 93–99, Feb. 2015.

(25) W. W. Lee, C.-S. Lu, C.-W. Chuang, Y.-J. Chen, J.-Y. Fu, C.-W. Siao, and C.-C. Chen, “Synthesis of bismuth oxyiodides and their composites: characterization, photocatalytic activity, and degradation mechanisms,” RSC Advances, vol. 5, no. 30, pp. 23450–23463, 2015.

(26) F. Cao, J. Wang, S. Li, J. Cai, W. Tu, X. Lv, and G. Qin, “Rapid room-temperature synthesis and visible-light photocatalytic properties of BiOI nanoflowers,” Journal of Alloys and Compounds, vol. 639, pp. 445–451, Aug. 2015.

(27) X. Xiao and W.-D. Zhang, “Facile synthesis of nanostructured BiOI microspheres with high visible light-induced photocatalytic activity,” Journal of Materials Chemistry, vol. 20, no. 28, p. 5866, 2010.

(28) Junhom C., “*In situ* Formation of Metal Nanoparticles (AgNPs) on Natural Rubber Latex Film thesis”, 2018.

(29) Liu, H. Li, N. Du, S. Song, and W. Hou, “Synthesis, characterization, and visible-light photocatalytic activity of BiOI hierarchical flower-like microspheres,” RSC Adv., vol. 4, no. 59, pp. 31393–31399, 2014.

Appendix

Experimental data

A.1 Element analysis using EDX technique

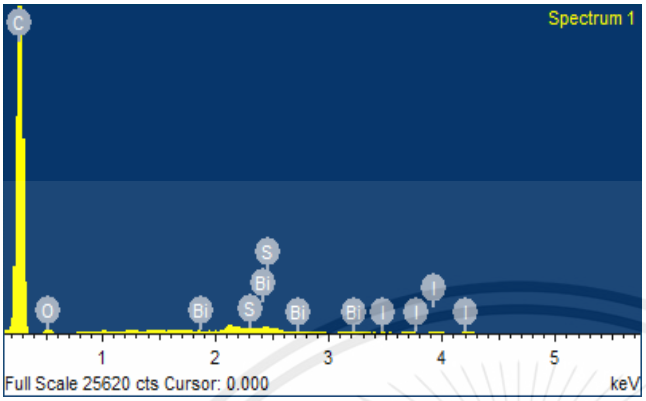

Element	Weight%	Atomic%
C K	93.11	96.66
O K	3.92	3.05
S K	0.19	0.07
I L	1.20	0.12
Bi M	1.58	0.09
Totals	100.00	

Figure A.1.1 EDX data of BiOI-coated on SPNR sheets using 1%wt of KI

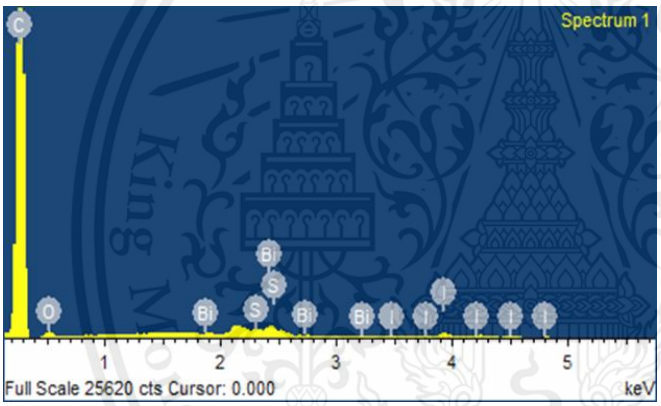

Element	Weight%	Atomic%
C K	92.04	96.16
O K	4.48	3.52
S K	0.19	0.08
I L	1.39	0.14
Bi M	1.89	0.11
Totals	100.00	

Figure A.1.2 EDX data of BiOI-coated on SPNR sheets using 2%wt of KI

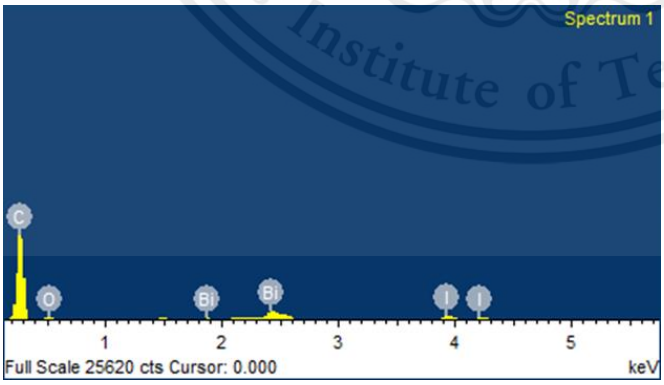

Element	Weight%	Atomic%
C K	79.75	93.51
O K	5.98	5.26
I L	6.03	0.67
Bi M	8.24	0.56
Totals	100.00	

Figure A.1.3 EDX data of BiOI-coated on SPNR sheets using 3%wt of KI

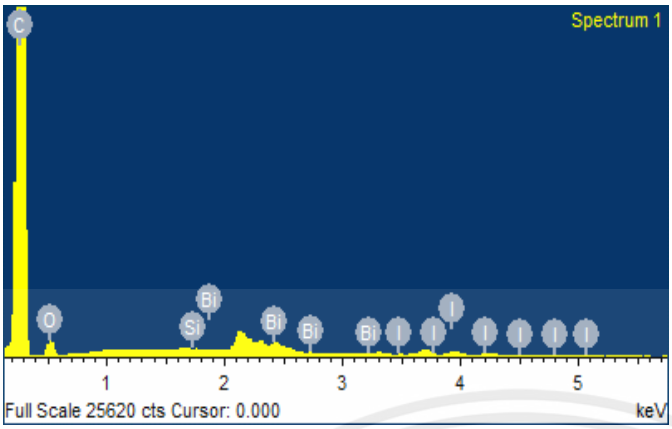

Element	Weight%	Atomic%
C K	91.67	94.54
O K	6.90	5.34
Si K	0.00	0.00
I L	0.83	0.08
Bi M	0.60	0.04
Totals	100.00	

Figure A.1.4 EDX data of BiOI-coated on SPNR by dipped into BiOI solution sheets using 1%wt of KI

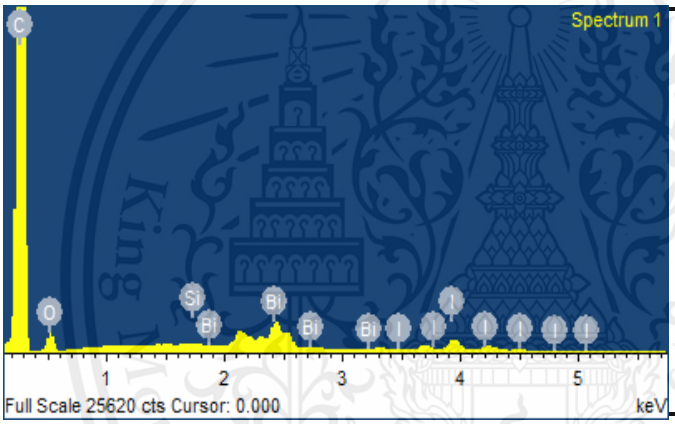

Element	Weight%	Atomic%
C K	86.94	93.50
O K	7.50	6.05
Si K	0.00	0.00
I L	2.48	0.25
Bi M	3.08	0.19
Totals	100.00	

Figure A.1.5 EDX data of BiOI-coated on SPNR by dipped into BiOI solution sheets using 2%wt of KI

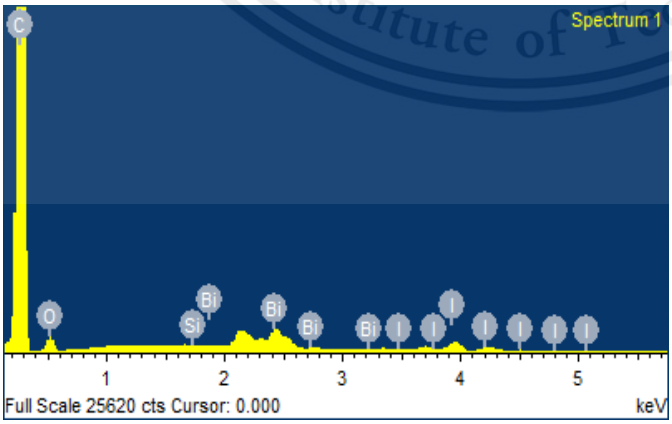

Element	Weight%	Atomic%
C K	88.79	94.39
O K	6.57	5.24
Si K	0.00	0.00
I L	2.11	0.21
Bi M	2.53	0.15
Totals	100.00	

Figure A.1.6 EDX data of BiOI-coated on SPNR by dipped into BiOI solution sheets using 3%wt of KI

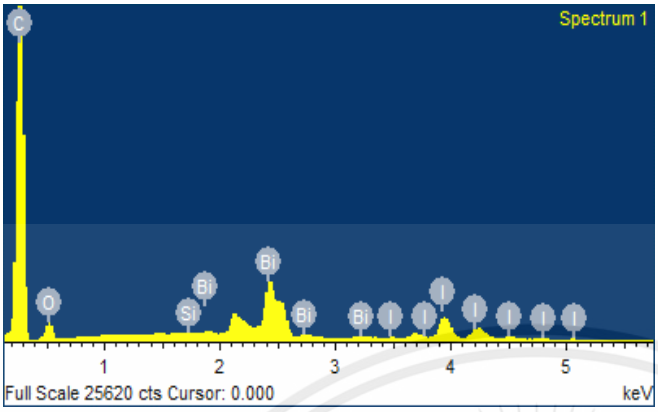

Element	Weight%	Atomic%
C K	74.92	91.87
O K	7.11	6.54
Si K	0.00	0.00
I L	7.01	0.81
Bi M	10.96	0.77
Totals	100.00	

Figure A.1.7 EDX data of BiOI-coated on SPNR sheets at pH 3

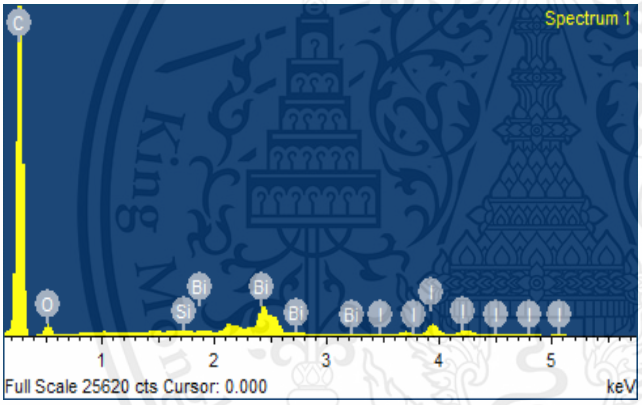

Element	Weight%	Atomic%
C K	80.79	92.76
O K	7.26	6.25
Si K	0.00	0.00
I L	4.67	0.51
Bi M	7.28	0.48
Totals	100.00	

Figure A.1.8 EDX data of BiOI-coated on SPNR sheets at pH 4

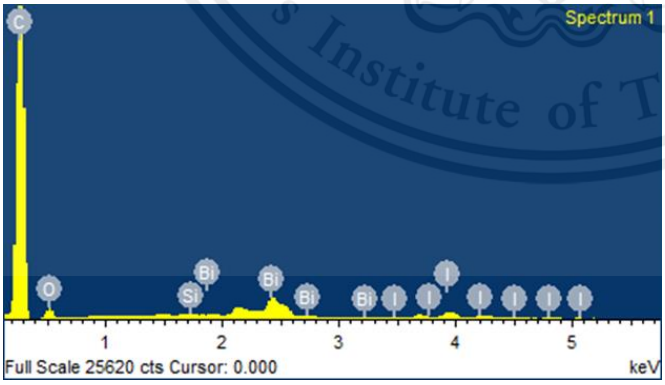

Element	Weight%	Atomic%
C K	85.60	93.53
O K	7.21	5.91
Si K	0.00	0.00
I L	2.64	0.27
Bi M	4.55	0.29
Totals	100.00	

Figure A.1.9 EDX data of BiOI-coated on SPNR sheets at pH 5

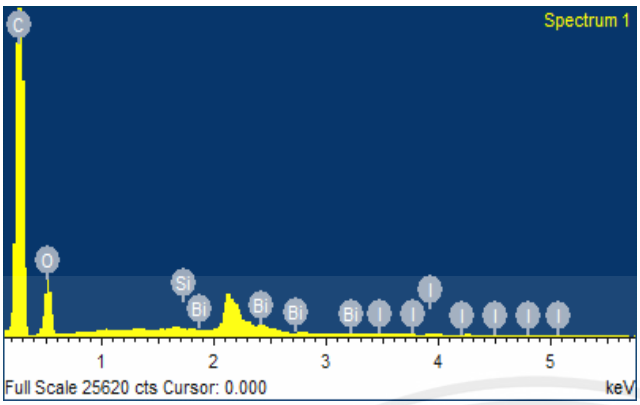

Element	Weight%	Atomic%
C K	75.29	80.97
O K	23.45	18.93
Si K	0.00	0.00
I L	0.40	0.04
Bi M	0.85	0.05
Totals	100.00	

Figure A.1.10 EDX data of BiOI/PMMA-modified SPNR sheets at 10 min of dipping time

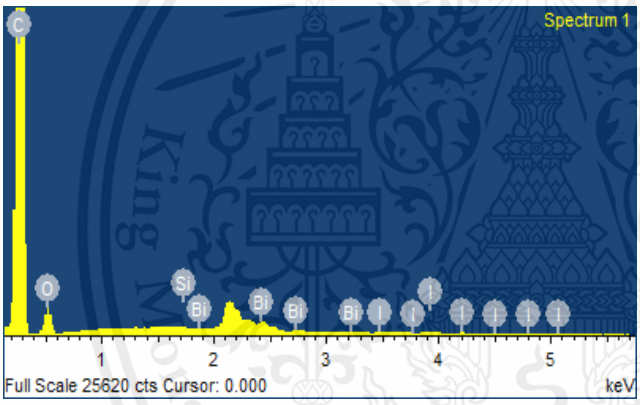

Element	Weight%	Atomic%
C K	86.52	90.48
O K	11.98	9.41
Si K	0.00	0.00
I L	0.50	0.05
Bi M	1.00	0.06
Totals	100.00	

Figure A.1.11 EDX data of BiOI/PMMA-modified SPNR sheets at 20 min of dipping time

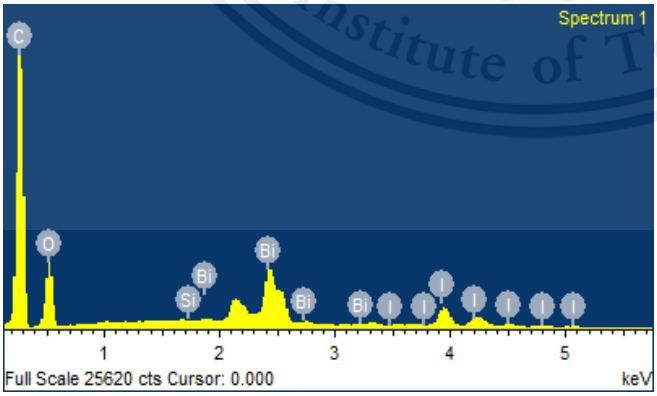

Element	Weight%	Atomic%
C K	58.72	75.41
O K	23.87	23.02
Si K	0.00	0.00
I L	6.14	0.75
Bi M	11.26	0.83
Totals	100.00	

Figure A.1.12 EDX data of BiOI/PMMA-modified SPNR sheets at 30 min of dipping time

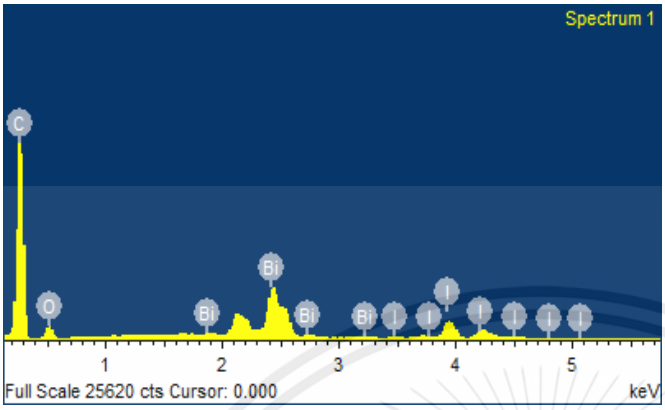

Element	Weight%	Atomic%
C K	66.57	90.08
O K	7.31	7.43
I L	9.19	1.18
Bi M	16.93	1.32
Totals	100.00	

Figure A.1.13 EDX data of BiOI/PMMA-modified SPNR sheets at 40 min of dipping time

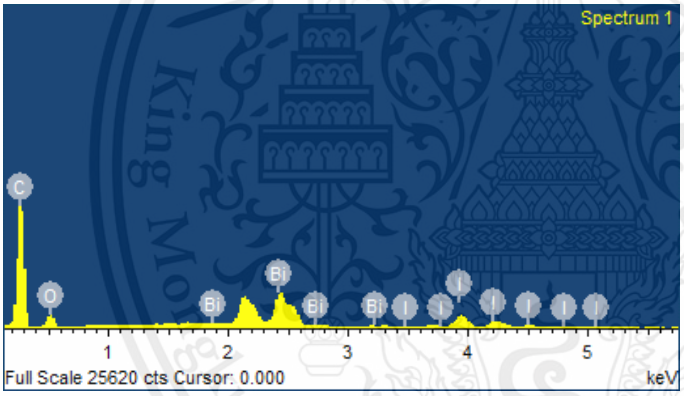

Element	Weight%	Atomic%
C K	62.51	85.92
O K	11.19	11.54
I L	9.11	1.18
Bi M	17.19	1.36
Totals	100.00	

Figure A.1.14 EDX data of BiOI/PMMA-modified SPNR sheets at 50 min of dipping time

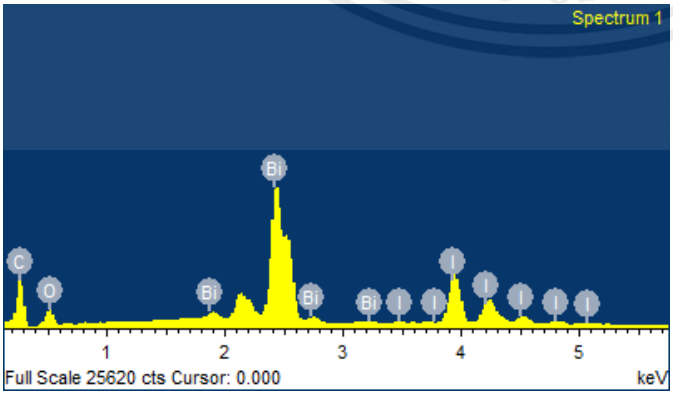

Element	Weight%	Atomic%
C K	22.72	70.50
O K	5.94	13.84
I L	25.50	7.49
Bi M	45.84	8.18
Totals	100.00	

Figure A.1.15 EDX data of BiOI/PMMA-modified SPNR sheets at 60 min of dipping time

A.2 The structure analysis using XRD pattern

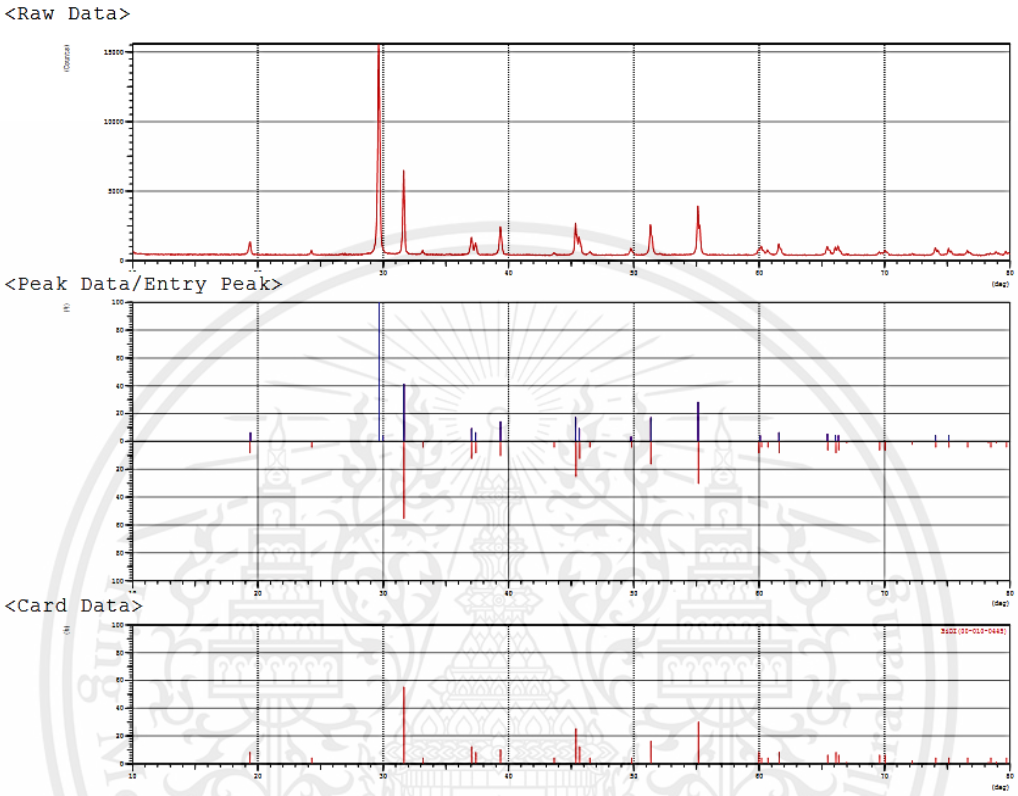

Figure A.2.1 XRD pattern of BiOI powder

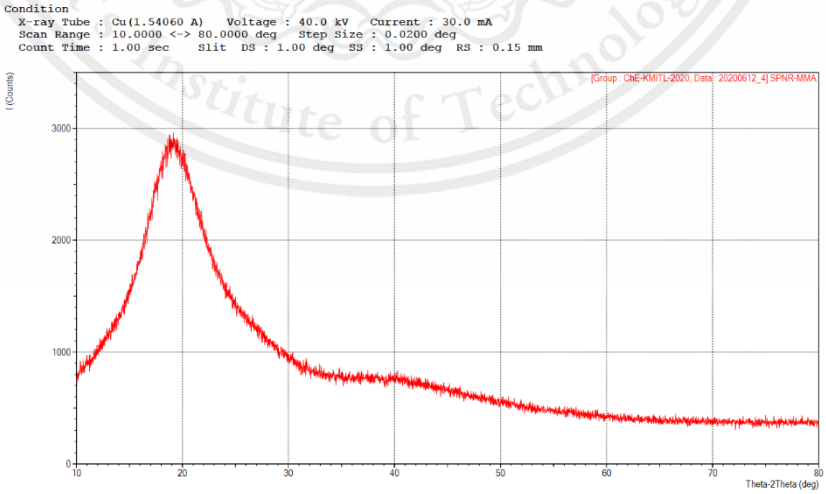

Figure A.2.2 XRD pattern of PMMA-modified SPNR

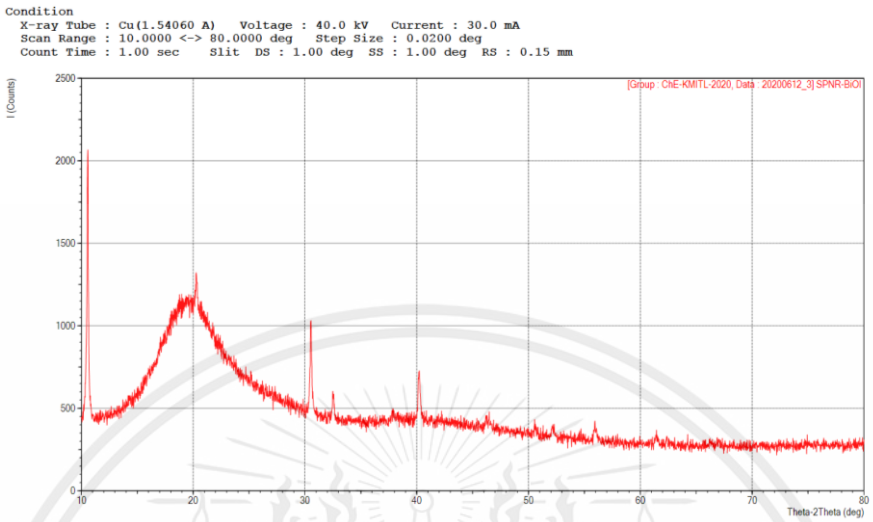

Figure A.2.3 XRD pattern of BiOI-coated SPNR

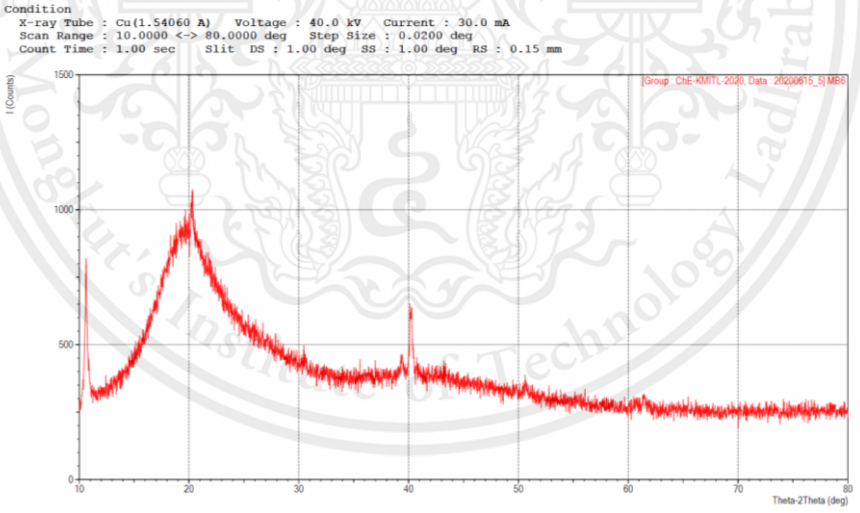

Figure A.2.4 XRD pattern of BiOI/PMMA-modified SPNR at 60 min of dipping time

A.3 TG measurement using thermogravimetric analyzer

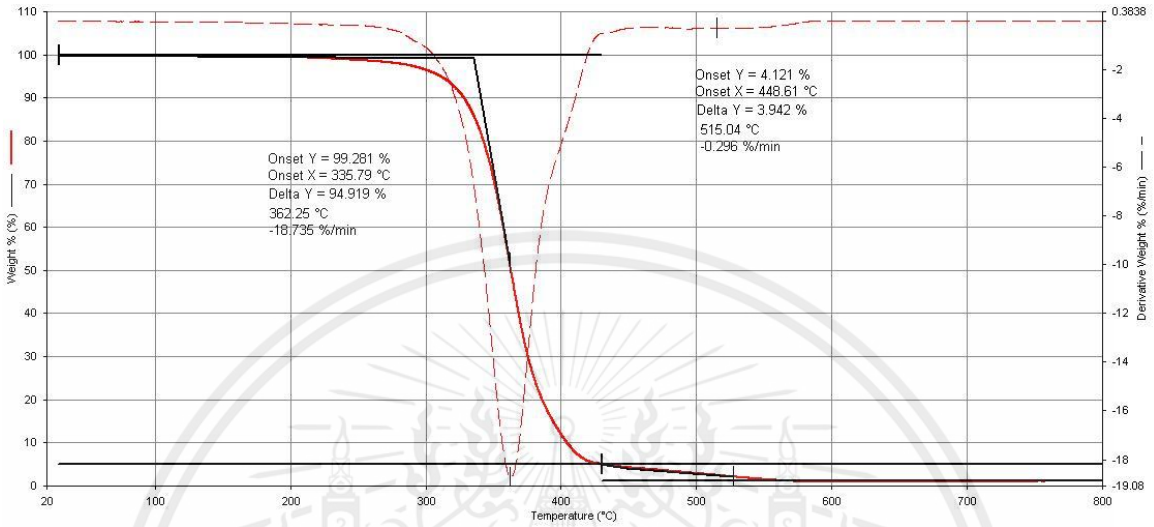

Figure A.3.1 TGA profiles of BiOI/PMMA-modified SPNR at 10 min of dipping time

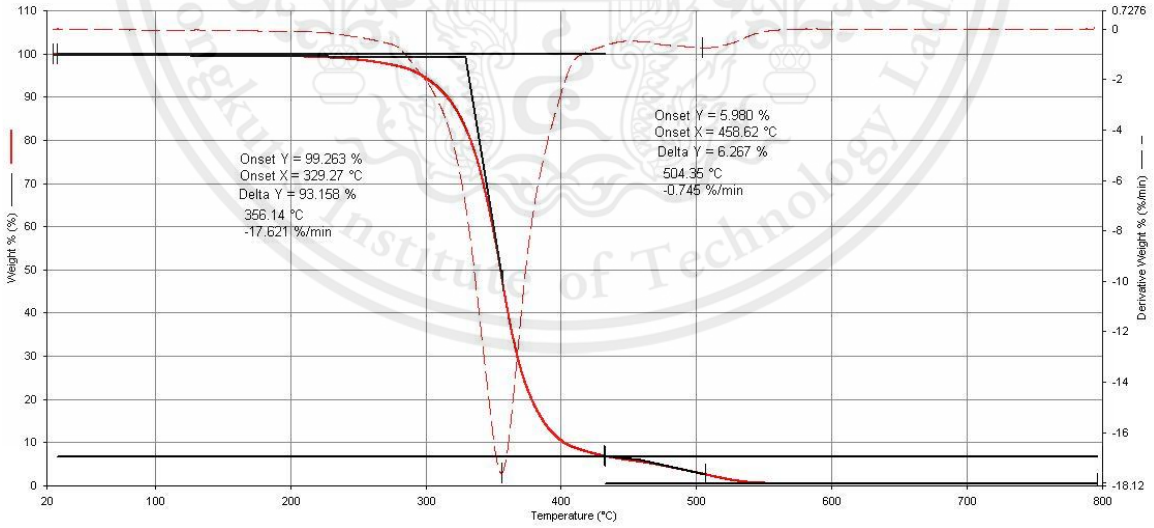

Figure A.3.2 TGA profiles of BiOI/PMMA-modified SPNR at 20 min of dipping time

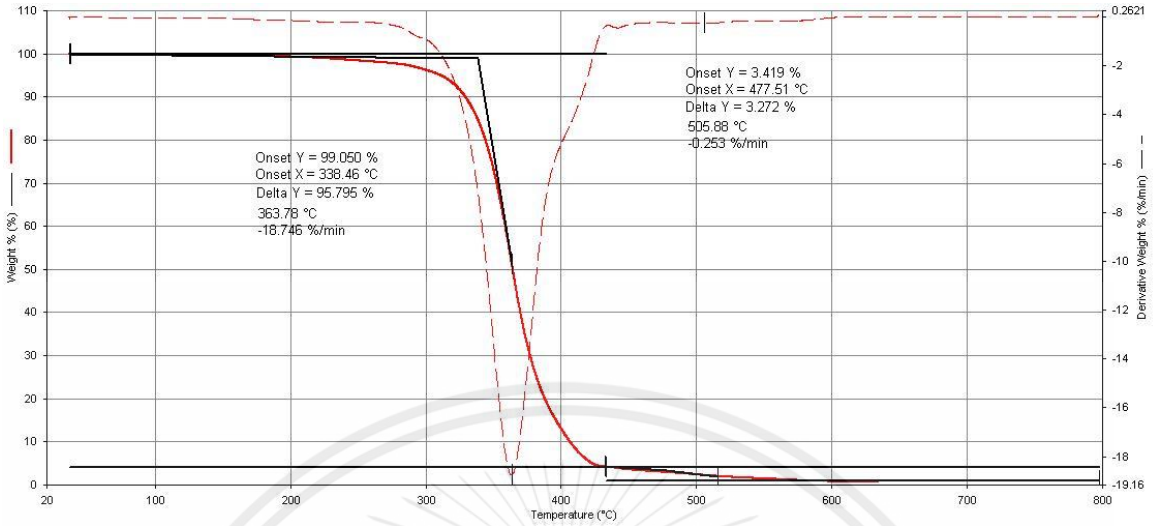

Figure A.3.3 TGA profiles of BiOI/PMMA-modified SPNR at 30 min of dipping time

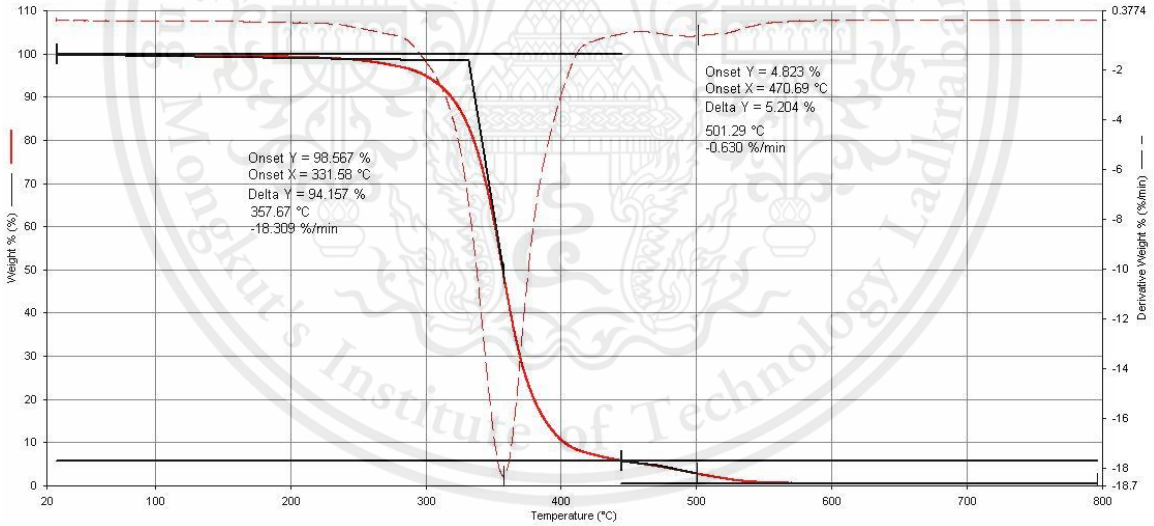

Figure A.3.4 TGA profiles of BiOI/PMMA-modified SPNR at 40 min of dipping time

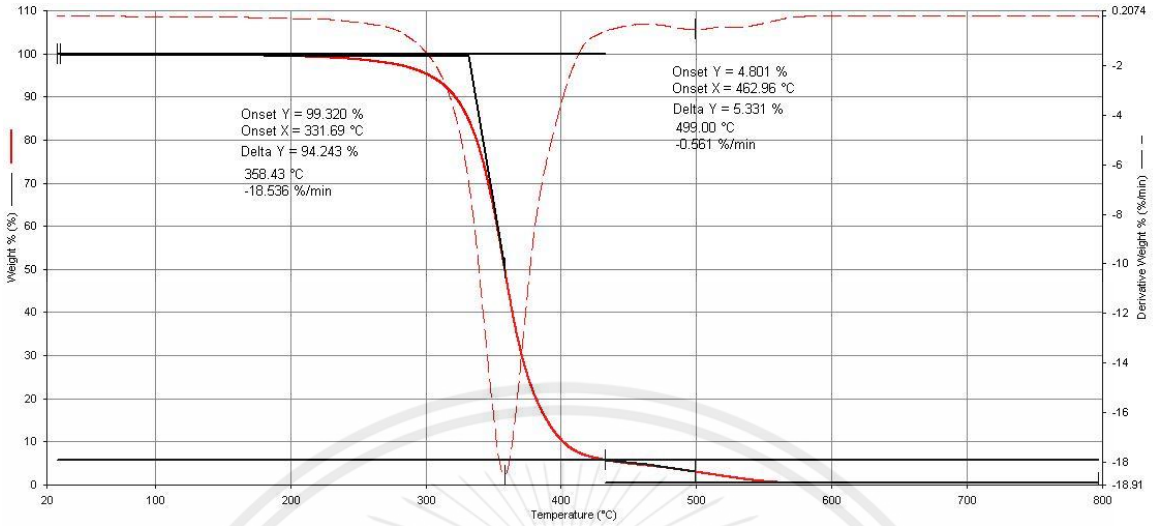

Figure A.3.5 TGA profiles of BiOI/PMMA-modified SPNR at 50 min of dipping time

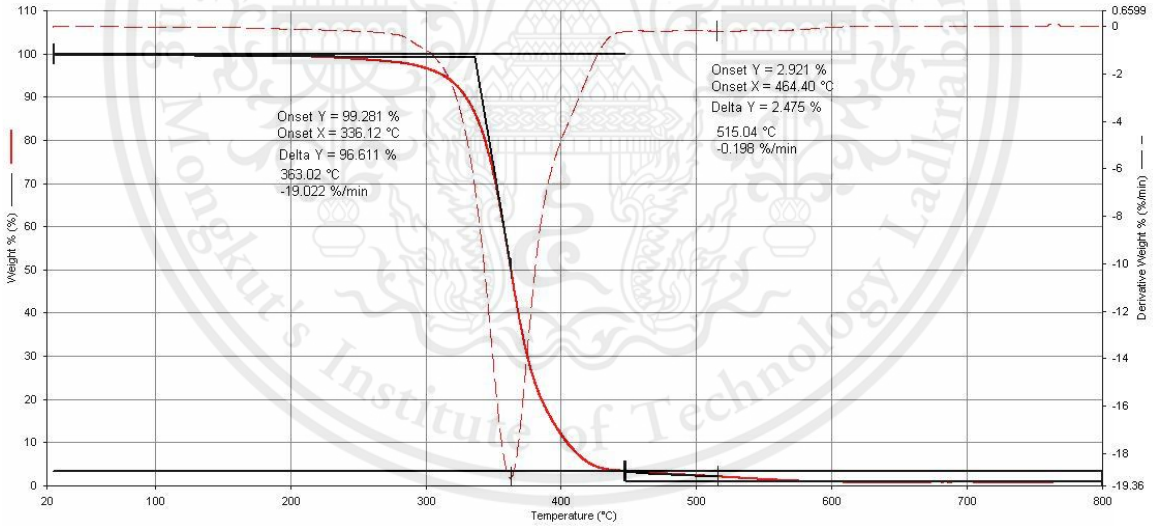

Figure A.3.6 TGA profiles of BiOI/PMMA-modified SPNR at 60 min of dipping time

A.4 Photodegradation data using FT-IR spectrum

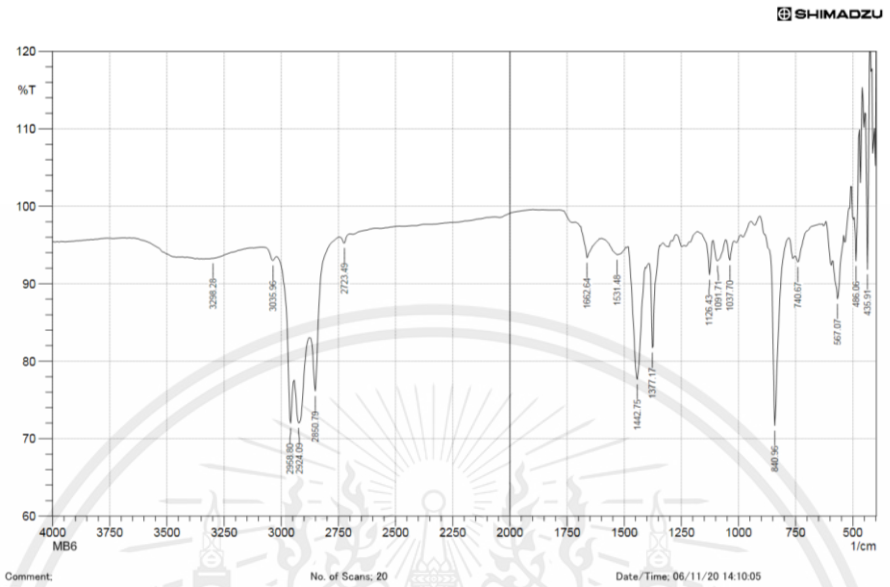

Figure A.4.1 FT-IR spectra of BiOI/PMMA-modified SPNR at 60 min

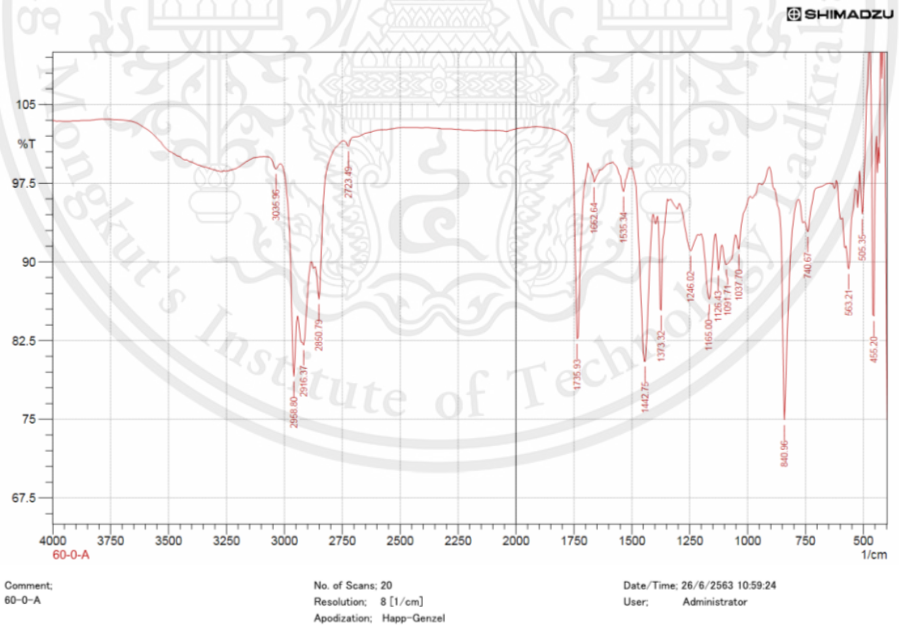

Figure A.4.2 FT-IR spectra of BiOI/PMMA-modified SPNR at 60 min with SA under UV-A irradiation for 0 h

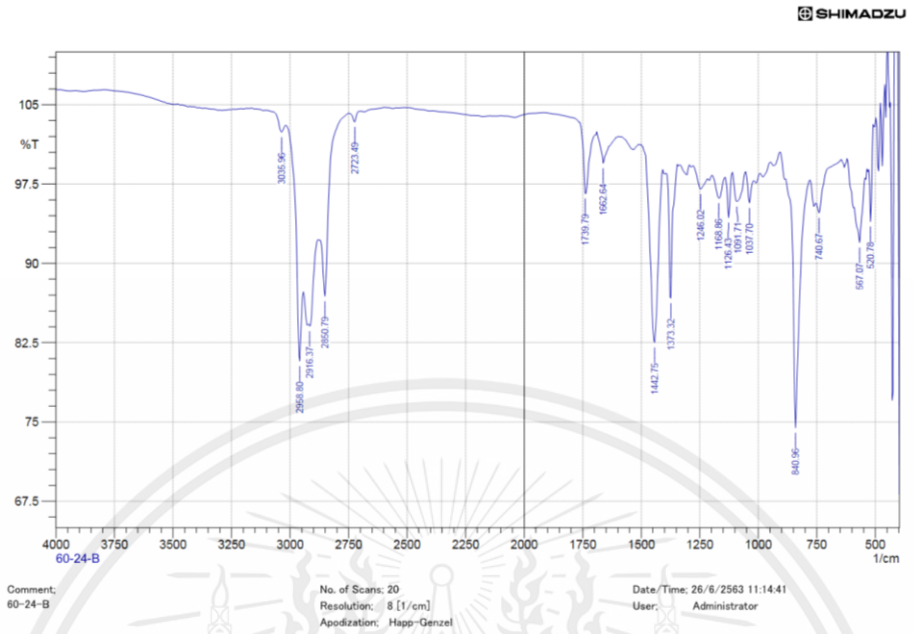

Figure A.4.3 FT-IR spectra of BiOI/PMMA-modified SPNR at 60 min with SA under UV-A irradiation for 24 h

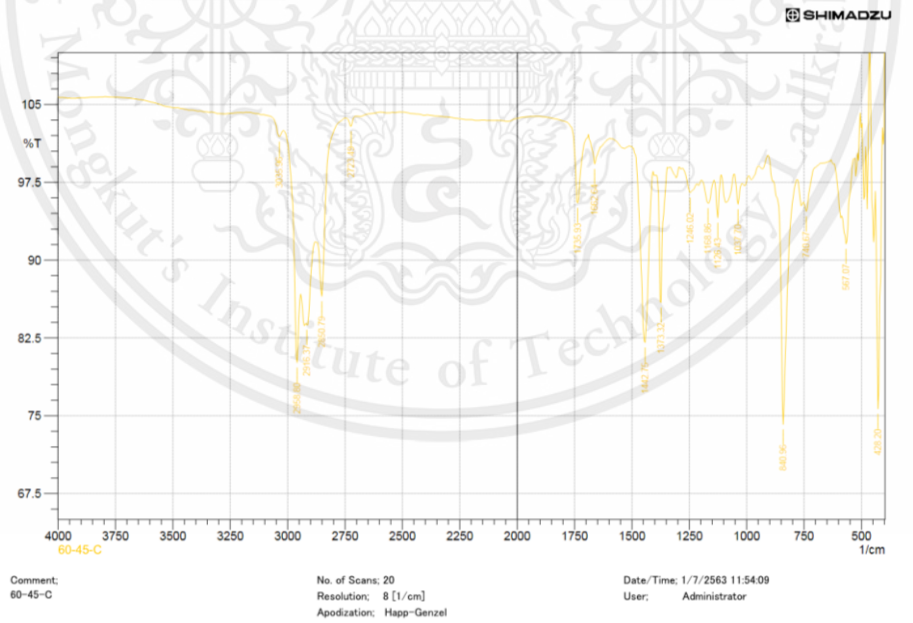

Figure A.4.4 FT-IR spectra of BiOI/PMMA-modified SPNR at 60 min with SA under UV-A irradiation for 45 h

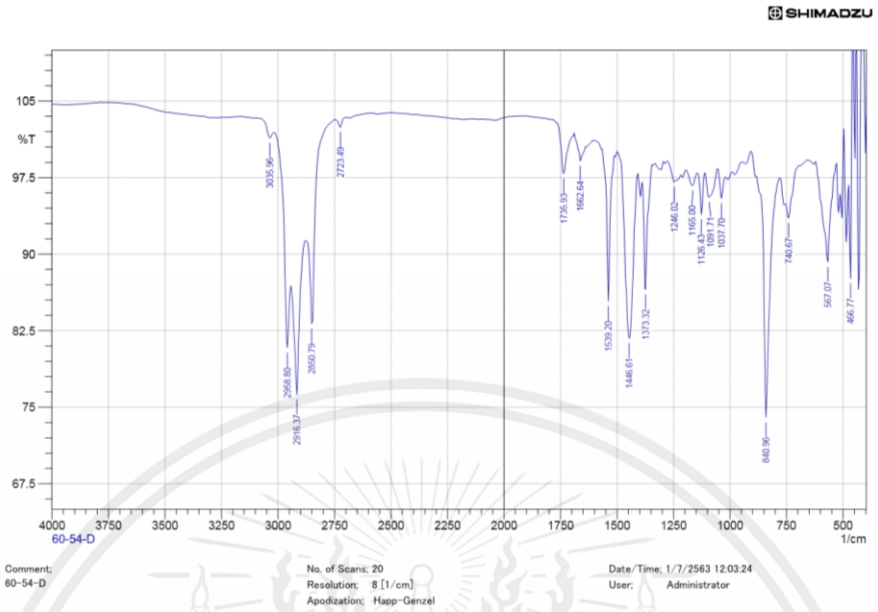

Figure A.4.5 FT-IR spectra of BiOI/PMMA-modified SPNR at 60 min with SA under UV-A irradiation for 54 h

Author Biography

Name:	Pathitta Kongthong
Date of Birth:	06/05/1997
Address:	289 Village No. 4, Khok sam rong sub-district, Khok sam rong district, Lopburi 15120
E-mail:	Pathitta_kt@hotmail.com
Academic Background:	Petrochemical Engineering, Department of Chemical Engineering, Faculty of Engineering, King Mongkut's Institute of Technology Ladkrabang
Working Experience:	Internship with Indorama ventures